1970

Optimizing diesel engine efficiency using the controllability of a variable ratio hydrostatic transmission

Gordon Wright

Department: Mechanical and Aerospace Engineering

OPTIMIZING DIESEL ENGINE EFFICIENCY USING THE CONTROLLABILITY OF A VARIABLE RATIO HYDROSTATIC TRANSMISSION

BY

GORDON WRIGHT, 1941-

A DISSERTATION

Presented to the Faculty of the Graduate School of the

UNIVERSITY OF MISSOURI - ROLLA

In Partial Fulfillment of the Requirements for the Degree

DOCTOR OF PHILOSOPHY

in

MECHANICAL ENGINEERING

1970

Advisor

ABSTRACT

A linear mathematical model of a diesel engine, hydrostatic transmission, and electric dynamometer system was developed. This model was used as an aid in designing a single input controller which regulates engine speed to optimize efficiency while maintaining constant transmission output speed under changing load conditions.

Compensation was necessary to stabilize the system because of positive feedback in the engine control system. The compensated system's response was compared to that which was predicted analytically.

The analytical model was then extended to design the control system parameters to operate the engine and transmission in a representative vehicle.

ACKNOWLEDGEMENT

The author would like to thank the following individuals and organizations as an expression of his appreciation for their contributions toward this investigation:

Dr. V. J. Flanigan, my advisor, whose assistance and advice guided me during this study.

The Mechanical and Aerospace Engineering Department, for providing the financial support.

Deere & Co., for the use of the diesel engine.

Sunstrand Foundation, for the hydrostatic transmission components.

Mr. R. D. Smith, for his help with the laboratory equipment.

My wife, Carole, and my family, whose faith and encouragement were invaluable.

TABLE OF CONTENTS

LIST OF ILLUSTRATIONS

Page

Figures

NOMENCLATURE

N_o = engine output speed (rpm)

N_p = pump shaft speed (rpm)

N_{in} = engine input speed (rpm)

N_{inc} = calculated engine input speed (rpm)

N_m = motor shaft speed (rpm)

N_{ms} = motor input speed setting (rpm)

N_{pr} = reference pump speed (rpm)

N_{mr} = reference motor speed (rpm)

T_1 = engine torque (ft-lbf)

T_p = pump torque (ft-lbf)

T_m = motor torque (ft-lbf)

T_{el} = external load torque (ft-lbf)

W_f = fuel flowrate (lbf/hr)

Q_p = pump flowrate (in^3/min)

Q_m = motor flowrate (in^3/min)

V_p = pump displacement (in^3/rev)

V_m = motor displacement (in^3/rev)

P_p = pump pressure rise (psig)

P_m = motor pressure drop (psig)

P = transmission pressure difference (psig)

P_r = reference pressure (psig)

R_o = transmission displacement ratio, V_p/V_m

R_i = transmission ratio lever input setting

D = derivative with respect to time (1/sec)

τ_1 = time constant of the fuel valve actuator (sec)

τ_2 = time constant of the engine (sec)

τ_t = ratio servomotor time constant (sec)

τ_{ta} = ratio actuator time constant (sec)

τ_{ga} = governor actuator time constant (sec)

$$C_2 = \left.\frac{\partial Z}{\partial N_{in}}\right|_r \quad \text{(in/rpm)}$$

$$C_4 = \left.\frac{\partial F_s}{\partial N_o}\right|_r \quad \text{(rpm-hr/lbf)}$$

$$C_6 = \left.\frac{\partial N_o}{\partial W_f}\right|_r \quad \text{(rpm-hr/lbf)}$$

$$C_8 = \left.\frac{\partial W_f}{\partial T_1}\right|_r \quad \text{(lbf/(hr-ft-lbf))}$$

Z = input to the governor spring (in)

F_s = force feedback in the governor spring (lbf)

K_s = the governor spring constant (lbf/in)

K_1 = fuel valve flow constant (lbf/(hr-lbf))

K_t = ratio controller gain constant (volts/rpm)

K_{ta} = ratio actuator gain constant (in/(sec-volt))

K_p = inverse slope of the optimum linear BSFC curve (rpm/(ft-lbf))

K_g = governor controller gain (volts/rpm)

K_{ga} = governor actuator gain constant (in/(sec-volt))

K_{gl} = governor input lever gain constant (rpm/in)

K_l = ratio input lever gain constant (1/in)

T_s = engine torque set point (ft-lbf)

E_t = transmission ratio controller output (volts)

E_g = governor controller output (volts)

J_d = dynamometer inertia (ft-lbf-sec^2)

J_e = engine inertia (ft-lbf-sec^2)

J_v = vehicle inertia (ft-lbf-sec^2)

EV_{pr} = pump volumetric efficiency at rated conditions

EV_{mr} = motor volumetric efficiency at rated conditions

EM_{pr} = pump mechanical efficiency at rated conditions

EM_{mr} = motor mechanical efficiency at rated conditions

The lower case variables denote the change in the instantaneous variables about a reference value.

n_o = change in engine speed (rpm)

n_p = change in pump shaft speed (rpm)

n_{in} = change in engine input speed setting (rpm)

n_{inc} = change in calculated engine input speed (rpm)

n_m = change in motor shaft speed (rpm)

n_{ms} = change in motor input speed setting (rpm)

t_l = change in engine torque (ft-lbf)

t_p = change in pump torque (ft-lbf)

t_{el} = change in external load torque (ft-lbf)

w_f = change in fuel flowrate (lbf/hr)

p = change in transmission pressure difference (psig)

r_o = change in transmission displacement ratio

r_i = change in transmission ratio lever input setting

x_t = change in movement of the ratio input lever (in)

x_g = change in movement of the governor input lever (in)

e_t = change in the ratio controller output voltage (volts)

e_g = change in the governor controller output voltage (volts)

I. INTRODUCTION

In the design of engine driven vehicles it is necessary to have a transmission which converts the output characteristics of the prime mover to the torque and speed requirements of the load. Usually this has been achieved by a mechanical transmission with a fixed number of output/input ratios, hence requiring the operator to choose the proper ratio and engine speed to meet the load demands. This results in a compromise both in performance and in efficiency because the engine is operating at maximum efficiency at only one point in each speed range. Also, making the decisions and executing the ratio changes and engine speed settings consumes a great deal of the operator's time. Walter W. Killough [1]*, vice president and executive head, Construction Equipment Division, International Harvester Co., said, concerning the next 10 years of development in Farm, Construction, and Industrial Machinery "....I think it's possible we will have automated the selection of gear ratios in order to use full horsepower of the engine at all times --- to keep the load factor high on the engine --- without relying on operator judgement."

The ideal transmission would change the engine output to a suitable form automatically, smoothly, and efficiently. The operator skill requisites would be decreased and he could devote more time to safety and increased productivity.

Because of a number of developments, infinitely variable transmissions, whose speed ratio can be changed continuously to cover a range of up to 10:1,

---

*Bracketed numbers denote references in bibliography.

are becoming practical for vehicular applications. These transmissions can be mechanical, electrical, hydraulic, or combinations such as hydro-mechanical and electro-mechanical. Regardless of the medium for transmitting the power, all these transmissions have one common characteristic not found in fixed ratio transmissions and that is controllability. If a suitable controller were designed, the performance of the infinitely variable transmission can approach that of the ideal transmission. This controller should maintain a desired output speed while changing engine speed and transmission ratio to deliver a smooth flow of power at maximum efficiency to meet changing load requirements. Dr. Warren E. Wilson [2], consulting engineer, Chicago, Ill., in an article for "Machine Design" said, "Hydrostatic transmissions can be at least as simple as a standard automotive transmission and can incorporate in an automatic transmission a control system to assure optimum steady-state fuel consumption and maximum acceleration when required. However, it is necessary to devise a control that relates the throttle and pump displacement in an appropriate manner."

Fig. 1 shows a representative torque speed plane of an internal combustion engine. For optimum efficiency the engine should be controlled to operate at the intersection of the required horsepower curve and the curve of maximum efficiency. If the horsepower level increases, the output speed of the engine must also increase. Therefore, in order to maintain a constant vehicle speed under changing loads the transmission ratio must be controlled to hold the speed constant.

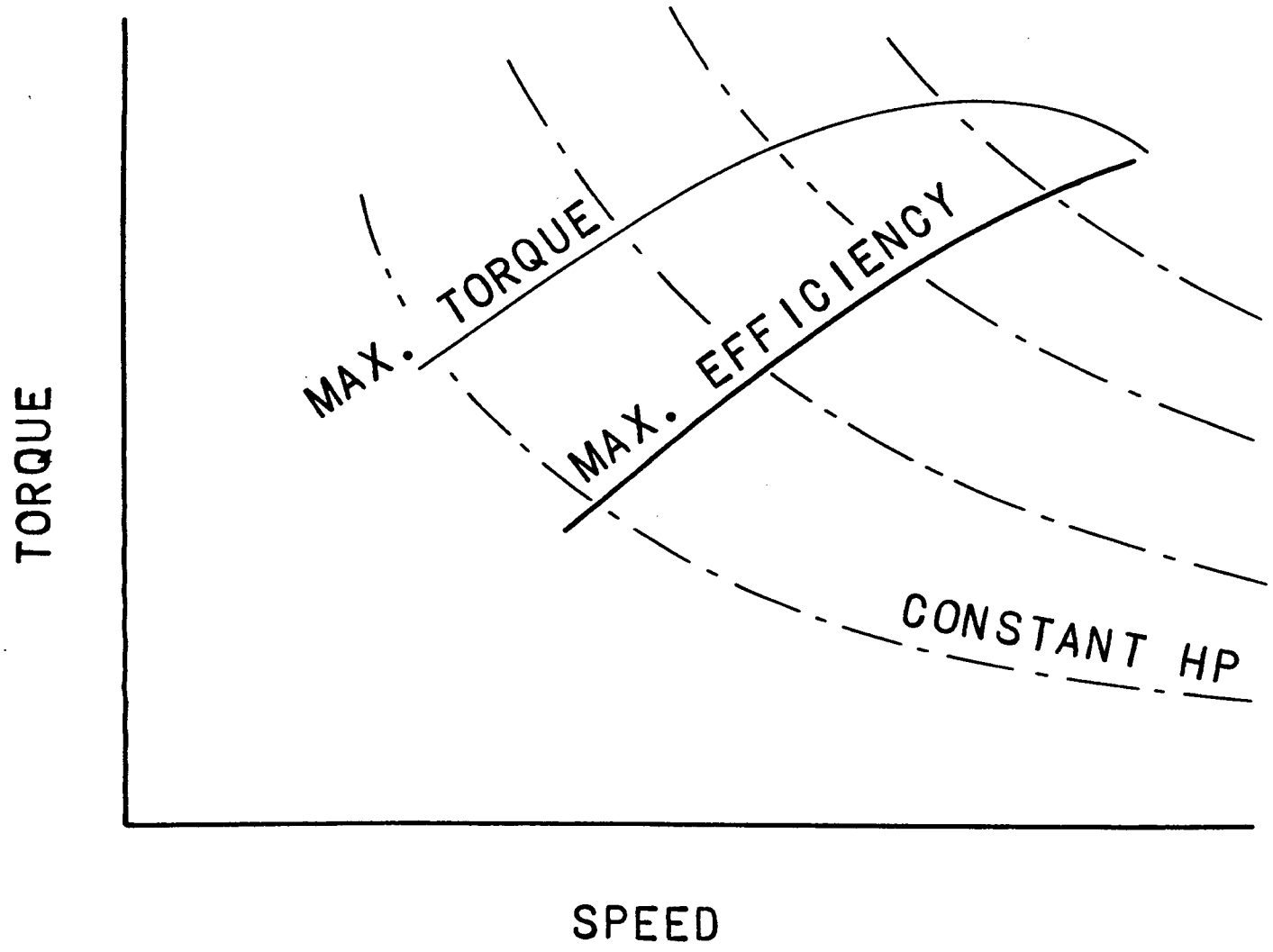

Figure 1. Maximum Engine Efficiency

It is the purpose of this work to design a single input controller which optimizes the efficiency of a diesel engine using the controllability of a variable ratio hydrostatic transmission and to investigate the steady-state and transient performance of the system.

II. REVIEW OF LITERATURE

In control system design it is useful to have a mathématical model of the system to be controlled. This model explains the inter-relationship of all the variables of the system, and can be used to analyze the control system design without resorting to the fabrication of components and laboratory tests. The complete model of a diesel engine and hydrostatic transmission would be a set of non-linear equations which would be difficult to analyze. But by defining reference points on the operating curve and considering small changes around these points, a linear model can be developed to approximate the non-linear system. The linear equations, although slightly inaccurate, will be sufficient to investigate the dynamic behavior of the system.

The linear mathematical model of a governor controlled engine given in Eq. (1) has been developed by Raven [3]. Capital letters are used to define instantaneous variables. Quantities with lower case letters denote the change of a variable about the reference operating condition. The linearized equation relating the change in output speed to the change in input speed signal and torque is:

$$n_o = \frac{C_2 C_6 K_1 K_s n_{in} - C_6 C_8 (1 + \tau_1 D) t_1}{(1 + \tau_1 D)(1 + \tau_2 D) + C_4 C_6 K_1} . \qquad (1)$$

Where the variables are

N_o = engine output speed (rpm)

N_{in} = engine input speed setting (rpm)

T_1 = engine torque (ft-lbf).

And the constants are

τ_1 = time constant of the fuel valve actuator (sec)

τ_2 = time constant of the engine (sec)

D = derivative with respect to time

$$C_2 = \frac{\partial Z}{\partial N_{in}} \Big|_r \text{ (in/rpm)}$$

Z = input to the governor spring (in)

$$C_4 = \frac{\partial F_s}{\partial N_o} \Big|_r \text{ (lbf/rpm)}$$

F_s = force feedback in the governor spring (lbf)

$$C_6 = \frac{\partial N_o}{\partial W_f} \Big|_r \text{ (rpm-hr/lbf)}$$

$$C_8 = \frac{\partial W_f}{\partial T_1} \Big|_r \text{ (lbf/(hr-ft-lbf)}$$

W_f = fuel flowrate (lbf/hr)

K_s = the governor spring constant (lbf/in)

K_1 = fuel valve flow constant (lbf/(hr-lbf)).

The equations describing the transmission components in terms of six characteristic coefficients which account for the losses have been developed by Dr. Warren E. Wilson [4, 5]. However, the determination of these constants requires several tests.

Another empirical development based upon manufacturer supplied data has been presented by Jack L. Johnson [6]. Because of the availability of

this data, equations (2) through (5) developed by Johnson were utilized in this work.

$$T_p = \frac{V_p P_p}{24\pi} + \frac{P_{pr} V_{pr} (1 - EM_{pr})}{24\pi N_{pr} EM_{pr}} N_p \tag{2}$$

$$Q_p = V_p N_p - V_{pr} N_{pr} \frac{(1 - EV_{pr})}{P_{pr}} P_p \tag{3}$$

$$Q_m = V_m N_m + V_{mr} N_{mr} \frac{(1 - EV_{mr})}{P_{mr} EV_{mr}} P_m \tag{4}$$

$$T_m = \frac{V_m P_m}{24\pi} - \frac{V_{mr} P_{mr} (1 - EM_{mr})}{24\pi N_{mr}} N_m \tag{5}$$

Where

T = torque (ft-lbf)

Q = oil flowrate (in^3/min)

V = displacement (in^3/rev)

P = pressure difference (psig)

N = shaft speed (rpm)

EV = volumetric efficiency

EM = mechanical efficiency.

The subscripts p and m denote quantities related to the pump and motor respectively. The subscript r indicates that the quantities are evaluated at rated conditions.

It has been recognized for more than a decade that the key to successful application of the hydrostatic transmission was proper control. A single

input controller which maintains a selected output speed while operating the engine at maximum efficiency has been recommended by several investigators.

D. F. Howson [7] in his experimental work with the N.I.A.E. PVMF (pump-variable-motor-fixed) hydrostatic tractor, demonstrated that for highest efficiency the governor setting should be the minimum that would provide the necessary power and the pump displacement be the maximum compatible with the desired motor speed. He concluded that a considerable fuel saving could result from proper control of both the engine and transmission and suggested that a single lever control system could be designed that would provide constant forward speed for a given lever position with the operation of the pump and engine linkage actuated by the load and lever setting.

Latson, Gordanier, Dargan, and Rio [8], in designing a control system for an army vehicle driven by a spark-ignition engine through a variable speed hydro-mechanical transmission, encountered a stability problem when using single lever control to maintain constant output speed while changing engine speed for maximum economy under varying loads. While changes were being made to eliminate the instability it was decided to use a control which held engine speed constant for an operator input signal and this signal had to be changed according to load variations to maintain constant output speed. This system was considered to be simpler and more economical to produce. However, this does not relieve the operator of the output speed regulation function.

A. L. Lebedev [9] also demonstrated that maximum efficiency for a PVMF hydrostatic tractor occurred with minimum governor setting and maximum pump displacement. He also compromised the single input control and

designed and tested a two lever control system which under part load and slow speeds increased the tractor efficiency by 10 to 12% over hand control. No mention is made of transient response or stability.

III. DISCUSSION

A. System Representation. The control system was to be designed to operate a John Deere "4020" diesel tractor engine driving a Sunstrand "22" series variable displacement pump and a "21" series fixed displacement motor. The load was to be applied by an electric dynamometer. Although this engine transmission combination was not optimal, the operating envelope was large enough to investigate the stability of the system over a representative region.

The block diagram representing the engine is presented in Figure 2. The engine model differs from the engine model described by Raven [3] only in the fact that the fuel control valve is operated directly by governor action without requiring servo assist, thus $\tau_1 = 0$. Therefore, for the engine under consideration

$$n_o = \frac{C_2 C_6 K_1 K_s n_{in} - C_6 C_8 t_1}{1 + \tau_2 D + C_4 C_6 K_1}. \tag{6}$$

The transmission equations were developed from equations (2) through (5) as follows. Since all the pump flow is directed to the motor

$$Q_p = Q_m .$$

And assuming the pressure drop in the lines is negligible compared to the pressure difference across the pump

$$P_p = P_m = P.$$

The transmission ratio will be one of the control variables, therefore, for convenience let

$$R_o = \frac{V_p}{V_m} .$$

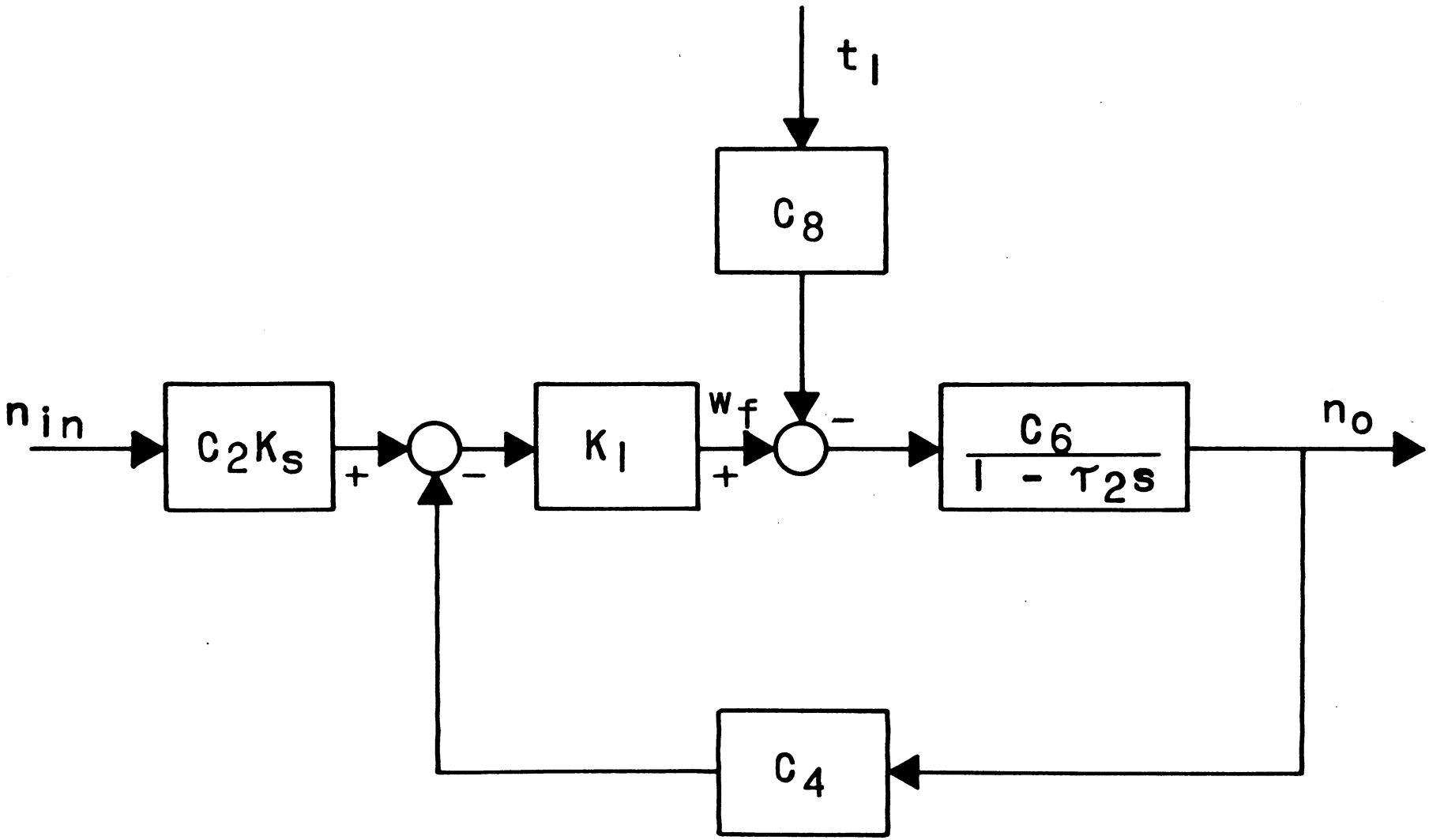

Figure 2. Diesel Engine Block Diagram

The output speed can now be found from Eq. (3) and (4).

$$N_m = R_o N_p - \left[\frac{V_{pr} N_{pr} (1 - EV_{pr})}{V_m P_r} + \frac{N_{mr} (1 - EV_{mr})}{P_r EV_{mr}} \right] P \qquad (7)$$

The pressure rise is found from Eq. (5)

$$P = \frac{24\pi T_m}{V_m} + \frac{P_{mr} (1 - EM_{mr})}{N_{mr}} N_m.$$

But the motor shaft torque T_m can be written as the sum of the external load torque and the torque required to accelerate the dynamometer.

$$T_m = T_{el} + \frac{2\pi}{60} J_d D N_m$$

Where:

T_{el} = external load torque (ft-lbf)

J_d = dynamometer inertia.

The pressure can now be related to the external torque and the output speed.

$$P = \frac{24\pi}{V_m} T_{el} + \left[\frac{P_r (1 - EM_{mr})}{N_{mr}} + \frac{2\pi 24\pi}{60 V_m} J_d D \right] N_m \qquad (8)$$

The pump torque can be rewritten as

$$T_p = \frac{V_m}{24\pi} R_o P + \frac{P_r V_{pr} (1 - EM_{pr})}{24\pi N_{pr} EM_{pr}} N_p \qquad (9)$$

The first term in both Eq. (7) and Eq. (9) is nonlinear since R_o, N_p, and P are variables. These equations can be linearized by the methods of Raven [3].

$$n_m = dN_m = \frac{\partial N_m}{\partial R_o}\Big|_r r_o + \frac{\partial N_m}{\partial N_p}\Big|_r n_p + \frac{\partial N_m}{\partial P}\Big|_r p$$

$$n_m = N_p r_o + R_o n_p - \left[\frac{V_{pr} N_{pr}(1 - EV_{pr})}{V_m P_r} + \frac{N_{mr}(1 - EV_{mr})}{P_r EV_{mr}}\right] p \tag{10}$$

Similiarly equations (8) and (9) are

$$p = \frac{24\pi}{V_m} t_{el} + \left[\frac{P_r(1 - EM_{mr})}{N_{mr}} + \frac{2\pi 24\pi}{60 V_m} J_d D\right] n_m \tag{11}$$

$$t_p = \frac{V_m P}{24\pi} r_o + \frac{V_m R_o}{24\pi} p + \frac{P_r V_{pr}(1 - EM_{pr})}{24\pi N_{pr} EM_{pr}} n_p. \tag{12}$$

These equations are represented in block diagram form in Fig. 3.

The Sunstrand "22" series pump is a swashplate controlled axial piston pump and, as is the case of most high pressure pumps, a servo motor is required to position the swashplate. The input lever is connected to the walking beam between the control valve and the swashplate by a spring which allows the operator to move the input lever to a new position rapidly with the swashplate following at a controlled rate. For small inputs this system obeys the basic equation of a first order system.

The input is related to the displacement ratio as

$$r_o = \frac{K_l x_t}{1 + \tau_t D} = \frac{r_i}{1 + \tau_t D}. \tag{13}$$

Where

x_t = movement of ratio input lever

τ_t = servo time constant

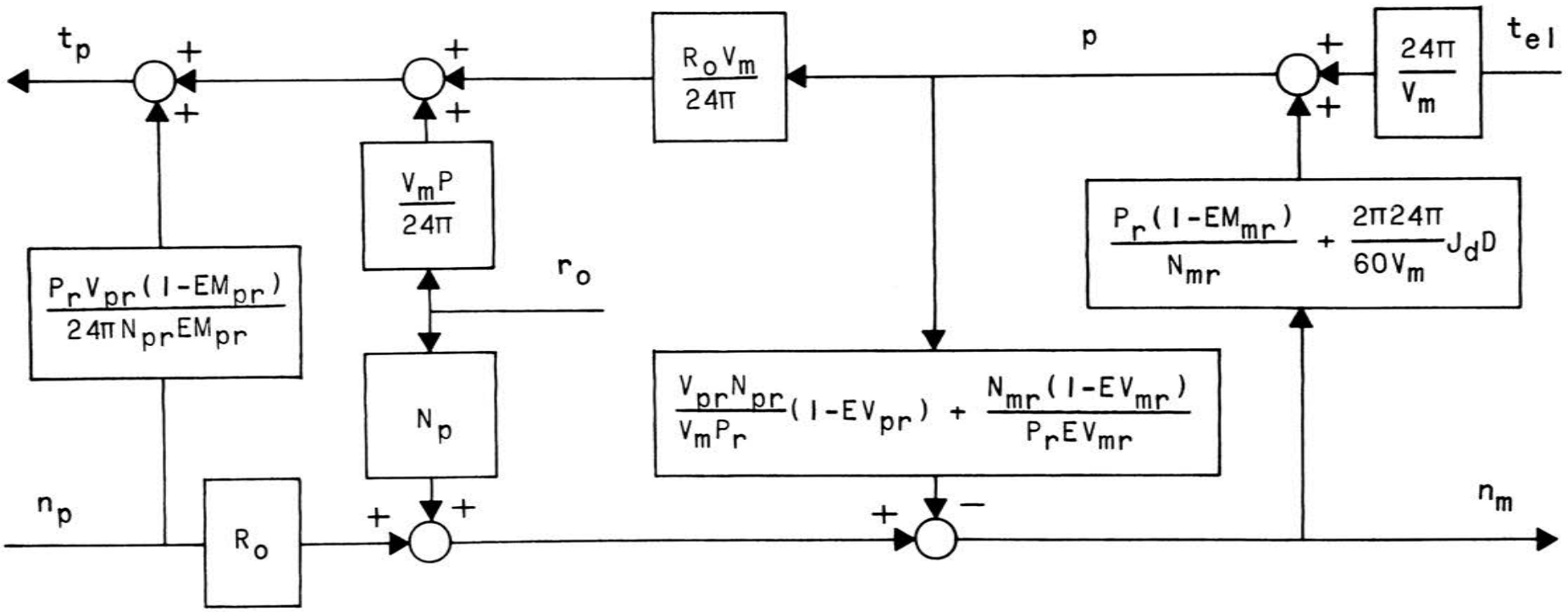

Figure 3. Hydrostatic Transmission Block Diagram

K_l = ratio input lever gain constant

r_i = ratio input.

The hydrostatic pump was directly coupled to the engine, therefore,

$$T_p = T_1$$

$$N_p = N_o.$$

The block diagrams for the engine, transmission, and ratio servomotor can now be connected as shown in Fig. 4.

From Fig. 1 it can be seen that the optimum speed is a function of torque, therefore, before the control system can be designed the optimum engine operating curve must be found. To accomplish this a series of constant speed variable torque runs were conducted according to SAE J816a Engine Test Code [10]. The data were corrected for atmospheric conditions and the torque, speed, fuel flowrate, brake horsepower (BHP), and brake specific fuel consumption (BSFC) were calculated.

The optimum curve was found by plotting BSFC versus BHP for each run. The minimum values of these curves were then plotted in the torque-speed plane of Fig. 5 as the minimum BSFC curve. Lines of constant BSFC were also plotted to help visualize the engine characteristics.

B. Control System Design. The controller must regulate the transmission ratio to maintain constant output speed while controlling the engine to operate along the minimum BSFC curve of Fig. 5. An integration in the ratio controller will be necessary to reduce steady-state output speed error to zero, therefore, the change in ratio can be written ideally as

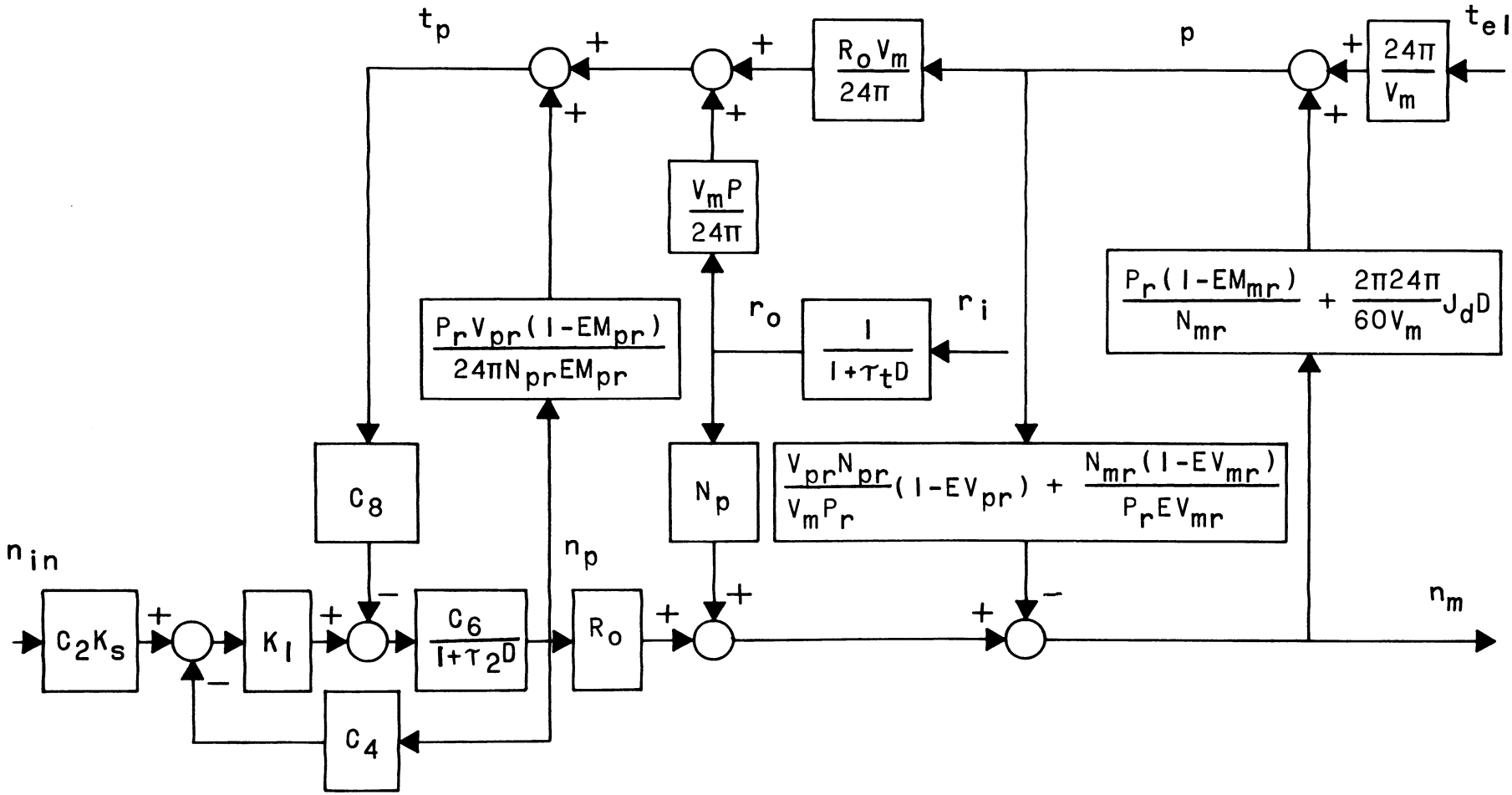

Figure 4. Engine-Transmission System Block Diagram

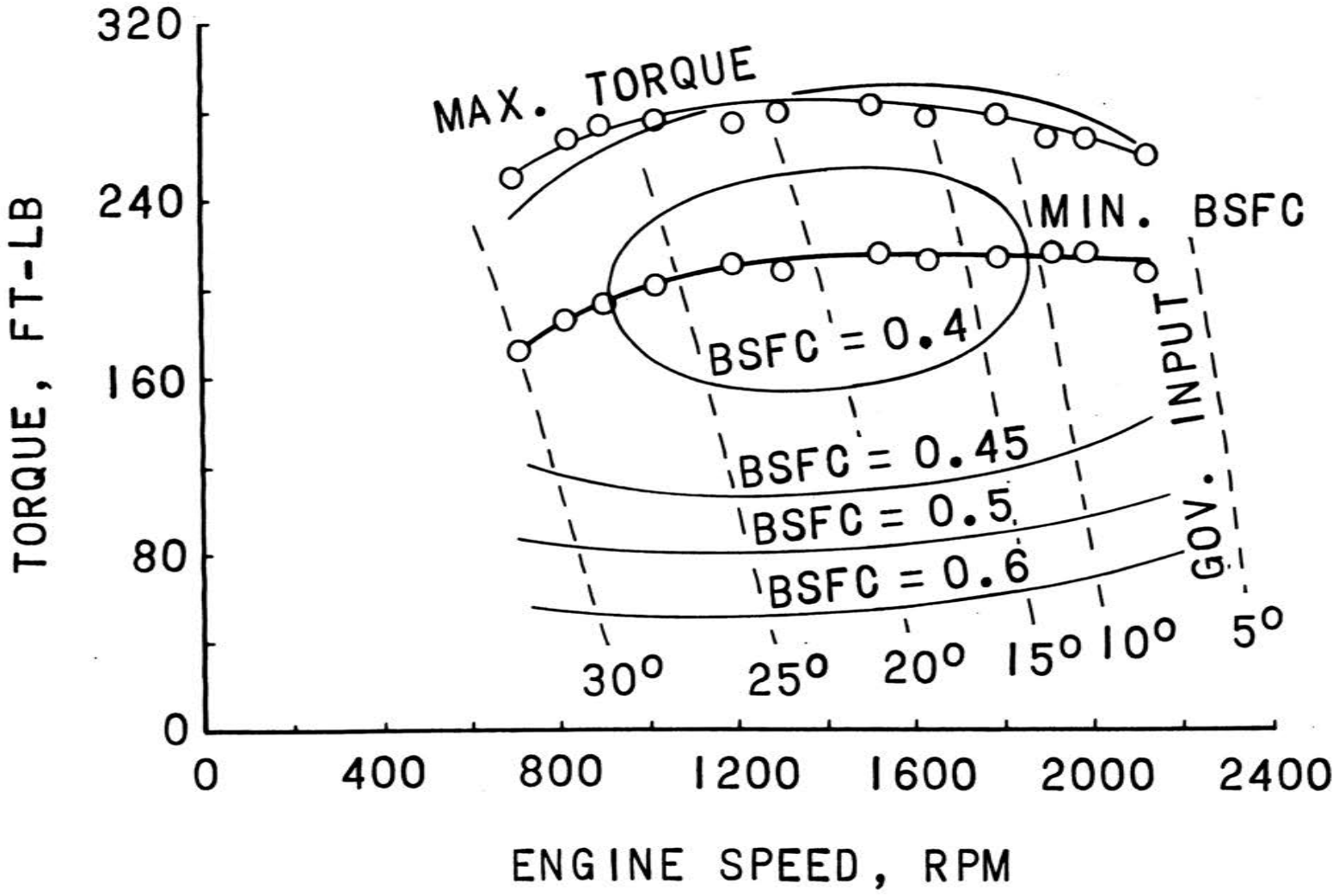

Figure 5. Minimum Brake Specific Fuel Consumption Curve

$$r_i = \frac{K_t}{D}(n_{ms} - n_m), \tag{14}$$

where

K_t = ratio controller gain constant

n_{ms} = output speed setting

n_m = output speed feedback.

The optimum engine speed in Fig. 5 is seen to be a non-linear function of torque. If this curve is approximated by a linear function the input speed can be controlled by engine torque. A proportional controller represented ideally by Eq. (15) would control the engine along a straight line in Fig. 5.

$$n_{inc} = K_p t_p \tag{15}$$

Where

n_{inc} = the calculated input speed setting

K_p = inverse slope of the optimum linear BSFC curve

$t_p = t_l$ = the engine and pump torque.

Eq. (14) and Eq. (15) represent the ideal control functions but the real actuators used to execute the control will have inertia, friction, and damping; therefore, the control components must be chosen and their characteristics included in the system representation before stability can be analyzed. Because of availability of components, electric motor operated linear actuators were used as final control elements to change the governor and transmission input settings. Neglecting the armature inductance and counter emf of the motor and the damping in the gear train the actuators are described by

$$x = \frac{K e}{D(1 + \tau D)} . \tag{16}$$

Where

x = output position of the actuator

K = gain constant

e = input voltage

τ = actuator time constant.

The equation for the real ratio actuator was developed by letting

$$e_t = K_t(n_{ms} - n_m) .$$

Where the subscript t refers to transmission ratio and from Eq. (16)

$$x_t = \frac{K_{ta} e_t}{D(1 + \tau_{ta} D)}$$

with the subscript ta denoting the ratio actuator. Therefore, from the relationship $r_i = K_l x_t$, the input to the ratio lever was

$$r_i = \frac{K_l K_{ta} e_t}{D(1 + \tau_{ta} D)} . \qquad (17)$$

Equation (15) yields the input speed setting. The error between the change in this calculated value from the reference point and the actual setting can be used to drive the governor actuator to the new position. The input voltage is

$$e_g = K_g(n_{inc} - n_{in})$$

with the subscript g referring to the governor. And from Eq. (16)

$$x_g = \frac{K_{ga} e_g}{D(1 + \tau_{ga} D)} .$$

The input speed was

$$n_{in} = K_{gl} x_g$$

$$n_{in} = \frac{K_{gl} K_{ga} e_g}{D(1 + \tau_{ga} D)} . \qquad (18)$$

Where

$$K_{gl} = \frac{\partial N_{in}}{\partial X_g}\Big|_r$$

K_{ga} = governor actuator gain constant.

The following equation was written by substituting for e_g and n_{inc}

$$n_{in} = \frac{K_{gl} K_{ga} K_g K_p t_p}{D(1 + \tau_{ga} D) + K_{gl} K_{ga} K_g} .$$

It was noted from Eq. (12) that t_p was a function of n_p and from Eq. (6) that n_p was a function of n_{in}. This relationship constituted a positive feedback loop and was recognized as a detriment to stable response. This condition was examined under section D.

C. Evaluation of Parameters. A reference condition must be specified for all the variables before the parameters can be evaluated. The engine speed range is from about 900 rpm to 2000 rpm. The center of the range will be the reference value.

$$N_p = N_{pr} = 1450 \text{ rpm}$$

The transmission ratio was chosen to be

$$R_o = 1.1 .$$

Before the pump torque and hence the transmission pressure rise was

specified, it was seen from Fig. 6 that for linear operation the pressure must be less than 4000 psig. To provide for a 10% increase in torque for transient response testing the reference pressure was 3600 psig, therefore, the pressure rise was the transmission pressure less the charge pump pressure* of 200 psig.

$$P_r = 3400 \text{ psig}$$

Now that P_r is specified, T_p can be found from Eq. (9) by substituting EM_{pr} from the manufacturer's performance data [11].

$$T_p = 166.11 \text{ ft-lbf}$$

The optimum T_p from Fig. 5 was 210 ft-lbf, therefore, the optimum torque would be out of the linear range of the pump. This is a result of a poor match between the transmission components and the engine. However, another line can be drawn through the point $N_p = 1450$ rpm and $T_p = 166.11$ ft-lbf with the same slope $1/K_p$. Although the operation of the engine will be less than optimal, the parameters of the engine will be changed only slightly and the stability of the system can be investigated.

The reference motor speed was evaluated from Eq. (7) by trial and error. A value for N_{mr} was selected and EV_{pr} and EM_{mr} were taken from the performance curves [11]. These efficiencies were substituted into Eq. (7) and N_m calculated. This value was used for a new N_{mr} and the process repeated until N_m did not change more than 2 rpm.

---

*The charge pump maintains a minimum of 200 psig in the transmission oil lines.

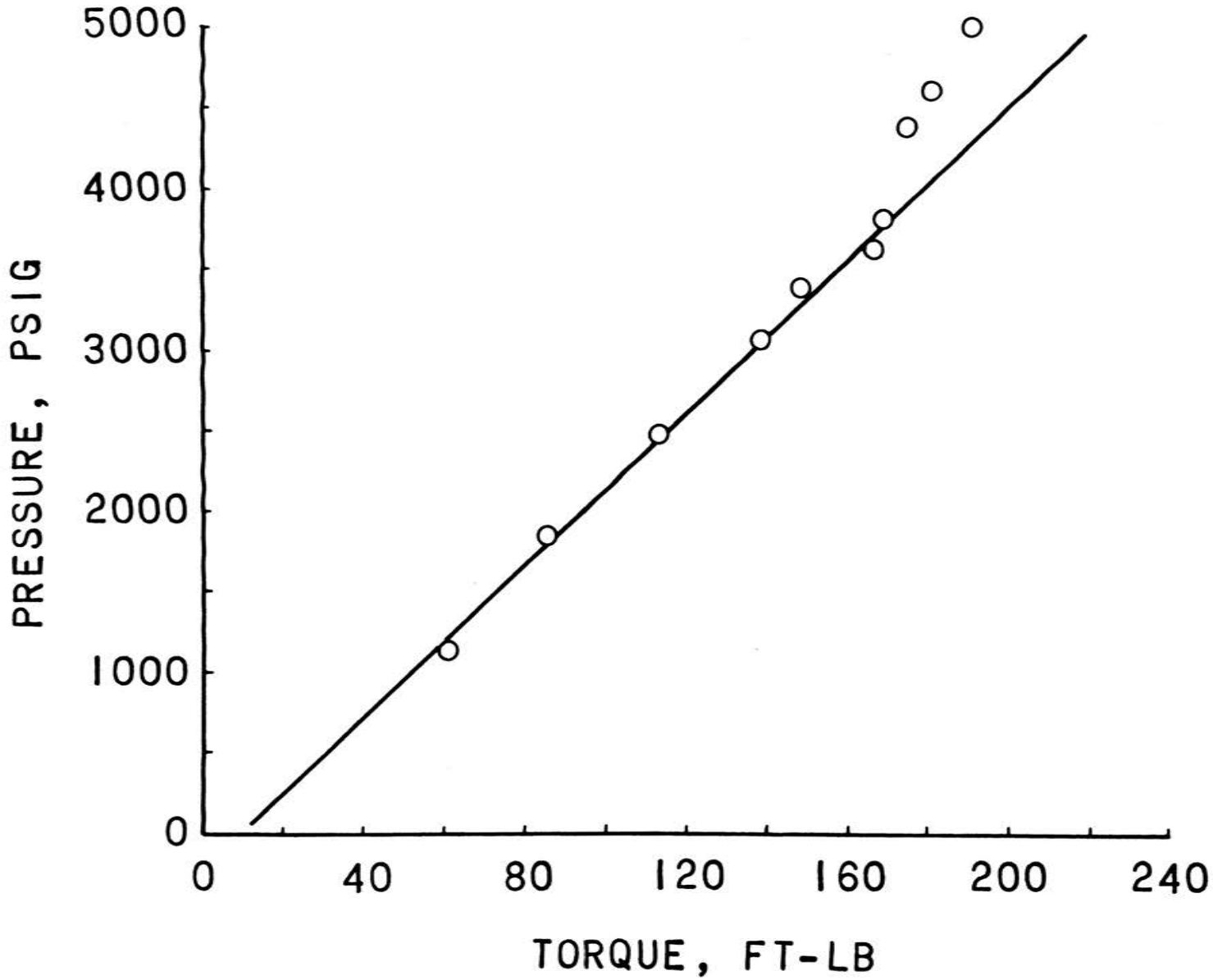

Figure 6. Transmission Pressure Characteristic

N_{mr} = 1452 rpm

The reference load torque was then calculated from Eq. (8).

T_{el} = 134.8 ft-lbf

The constants in Eq. (6) were evaluated through several tests. The governor spring constant K_s was found by removing the spring and measuring the deflection for a given load. This value was K_s = 11.3 lbf/in. The engine time constant was evaluated from the frequency response plot of Fig. 7. This data was taken with the engine connected to the transmission and the ratio set at zero while the governor input was a 10% peak to peak sinusoid around the reference condition of 1450 rpm. The closed loop engine time constant was 0.159 sec. with the open loop time constant, τ_2 = 1.124 sec. The remaining constants C_2, C_4, C_6, C_8, and K_1 were found through steady-state analysis.

The steady-state operating characteristic curves for the engine were obtained from the data recorded from the constant speed tests mentioned earlier. A family of curves of fuel flowrate versus torque for each constant speed run were plotted in Fig. 8. The values of fuel flowrate and speed at the intersection of the constant speed curves and lines of constant torque were plotted in Fig. 9. These are the steady-state operating characteristics of the engine.

To determine the governor characteristic curves the input speed setting was held constant and the speed and torque recorded at different torque settings. The broken lines of Fig. 5 were plotted from this data and are the governor droop lines. Values of speed at the intersection of the droop lines and lines of constant torque were plotted on the constant torque lines of Fig. 9 to

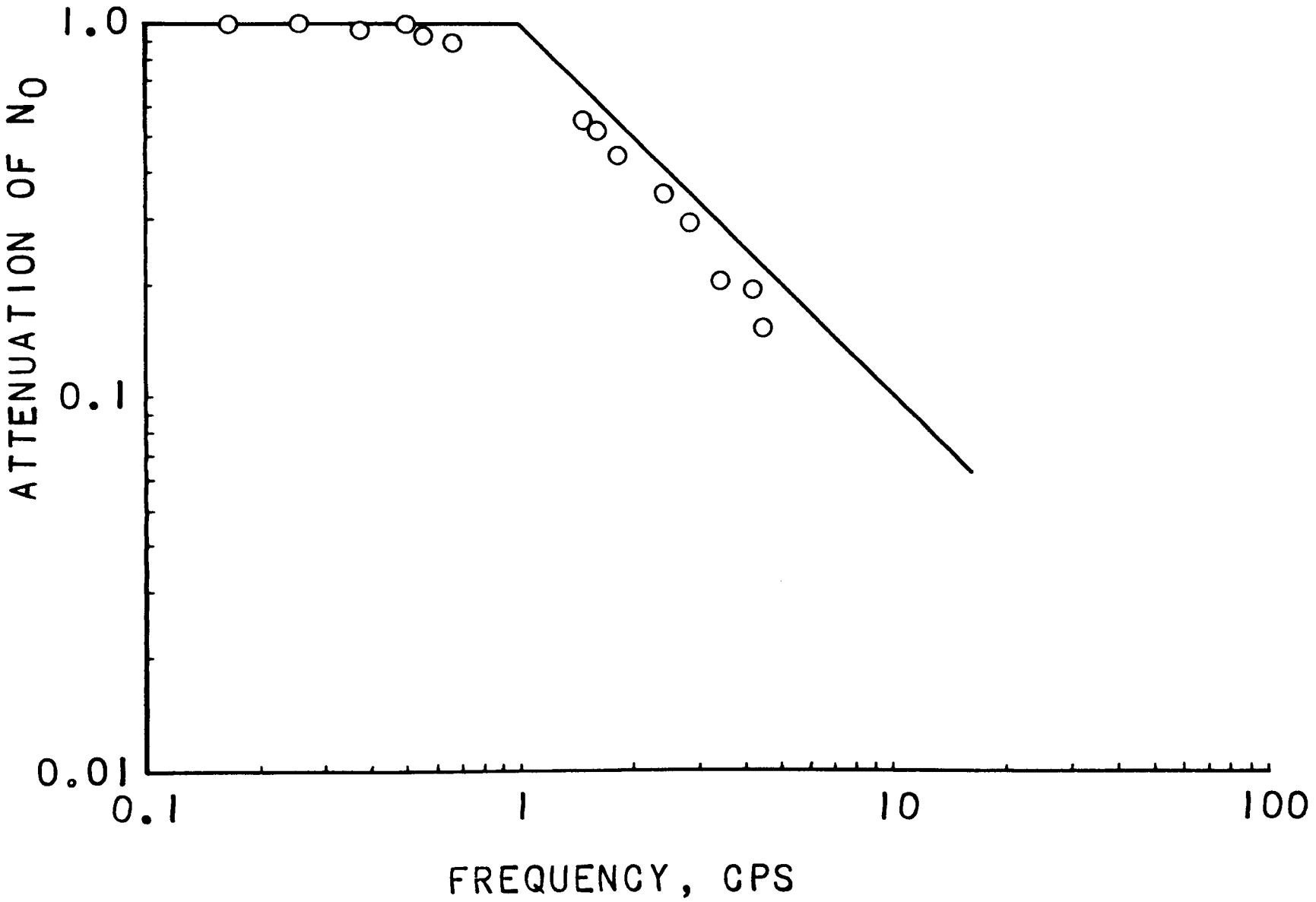

Figure 7. Diesel Engine Frequency Response

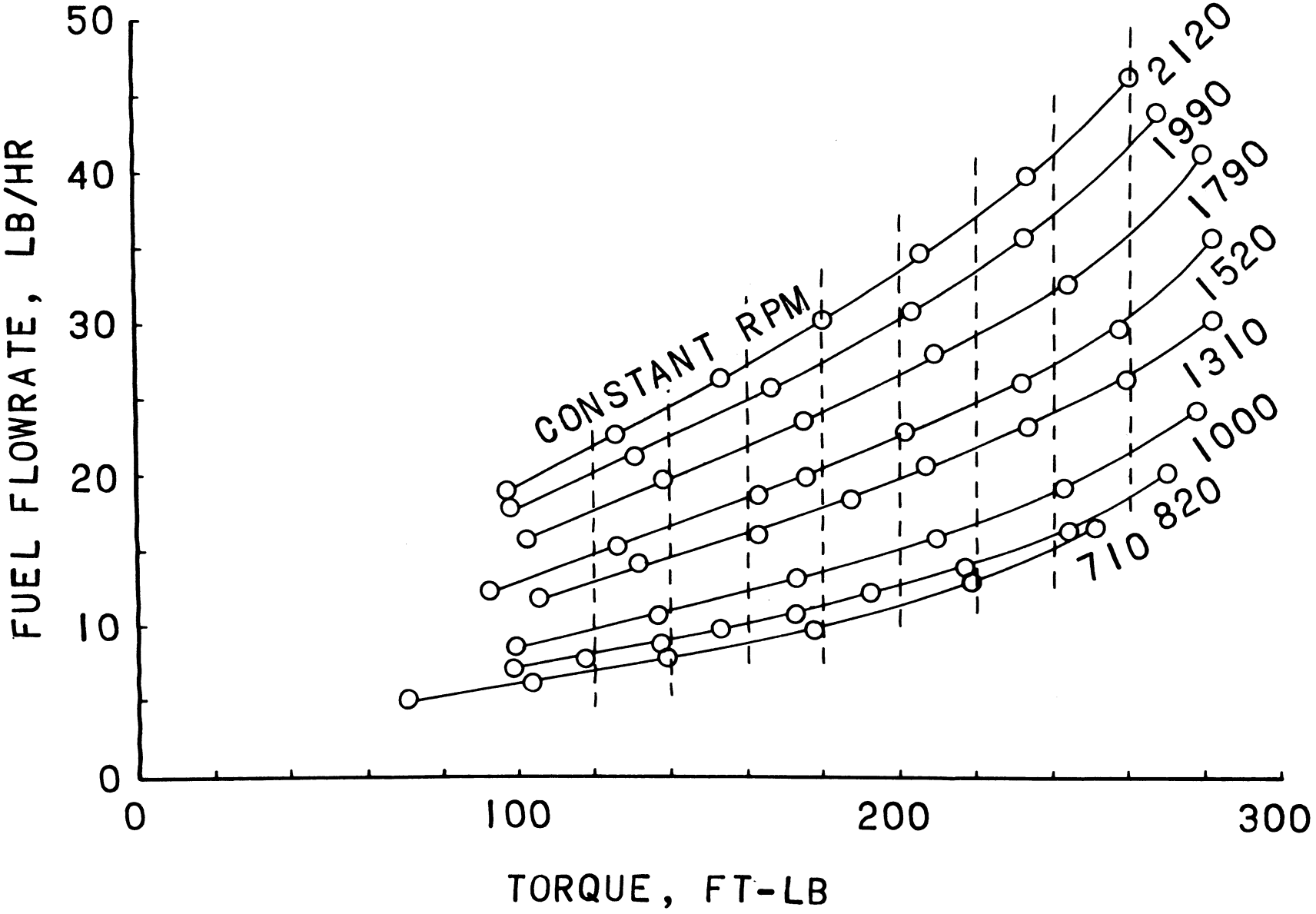

Figure 8. Method of Establishing Engine Steady-State Operating Characteristics

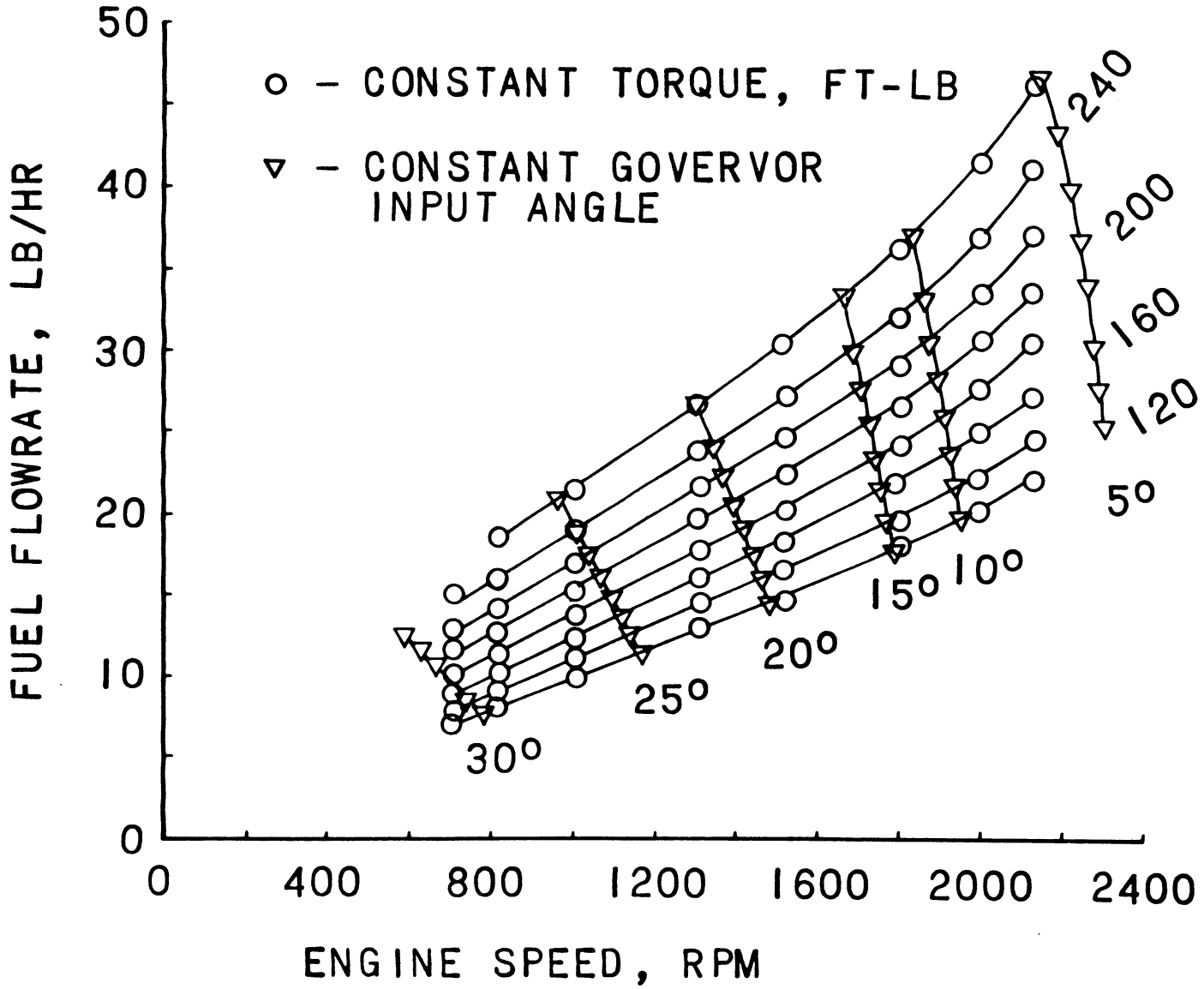

Figure 9. Engine and Controller Steady-State Operating Characteristic Curves

produce the governor steady-state operating characteristics.

From the block diagram of Fig. 2 the following equation can be written at steady-state

$$n_o = C_6 (w_f - C_8 t_1)$$

$$C_6 = \frac{\partial N_o}{\partial W_f}\Big|_{T_1}.$$

This derivative is evaluated graphically from Fig. 9.

$$C_6 = \frac{\partial N_o}{\partial W_f}\Big|_{T_1} = \frac{1600 - 1150}{20 - 14.5} = 81.8 \text{ rpm-hr/lbf}$$

And if

$$w_f = \frac{n_o}{C_6} + C_8 t_1$$

then from Fig. 9

$$C_8 = \frac{\partial W_f}{\partial T_1}\Big|_{N_o} = \frac{23.5 - 14}{220 - 120} = 0.095 \text{ lbf/(hr-ft-lbf)}$$

Similarly at steady-state Eq. (6) is

$$n_o = \frac{C_2 C_6 K_1 K_s}{1 + C_4 C_6 K_1} n_{in} - \frac{C_6 C_8}{1 + C_4 C_6 K_1} t_1$$

or

$$n_o = dN_o = \frac{\partial N_o}{\partial N_{in}}\Big|_{\substack{n \\ T_1^n}} + \frac{\partial N_o}{\partial T_1}\Big|_{N_{in}} t_1 .$$

From Fig. 9

$$\frac{\partial N_o}{\partial N_{in}}\Big|_{T_1} = \frac{C_2 C_6 K_1 K_s}{1 + C_4 C_6 K_1} = \frac{1750 - 1120}{15^o - 25^o}$$

N_{in} can be converted from degrees of rotation of the governor shaft to input speed in rpm by Fig. 10, a plot of shaft position versus idle speed.

$$\frac{\partial N_o}{\partial N_{in}}\Big|_{T_1} = \frac{C_2 C_6 K_1 K_s}{1 + C_4 C_6 K_1} = \frac{1750 - 1120}{1910 - 1340} = 1.1 \tag{19}$$

$$\frac{\partial N_o}{\partial T_1}\Big|_{N_{in}} = \frac{- C_6 C_8}{1 + C_4 C_6 K_1} = \frac{1390 - 1510}{220 - 120} = -1.2 \frac{\text{rpm}}{\text{ft-lbf}} \tag{20}$$

By measuring the length of the governor input lever to the spring, $r = 0.825$ in., C_2 can be determined

$$C_2 = \frac{\partial Z}{\partial N_{in}}\Big|_i$$

knowing that for small values of θ

$$z = r\theta$$

$$\frac{\partial Z}{\partial N_{in}}\Big|_i = r \frac{\partial \theta}{\partial N_{in}}\Big|_i .$$

The partial derivative of θ with respect to N_{in} can be measured from Fig. 10.

$$C_2 = \frac{\partial Z}{\partial N_{in}}\Big|_i = r \frac{\partial \theta}{\partial N_{in}}\Big|_i = 0.825 \left(\frac{30^o - 10^o}{1020 - 2260}\right) \frac{\pi}{180^o} = 0.000229 \frac{\text{in}}{\text{rpm}} .$$

Solving for the quantity $(1 + C_4 C_6 K_1)$ in Eq. (19) and Eq. (20) and equating the two expressions the constant K_1 was found.

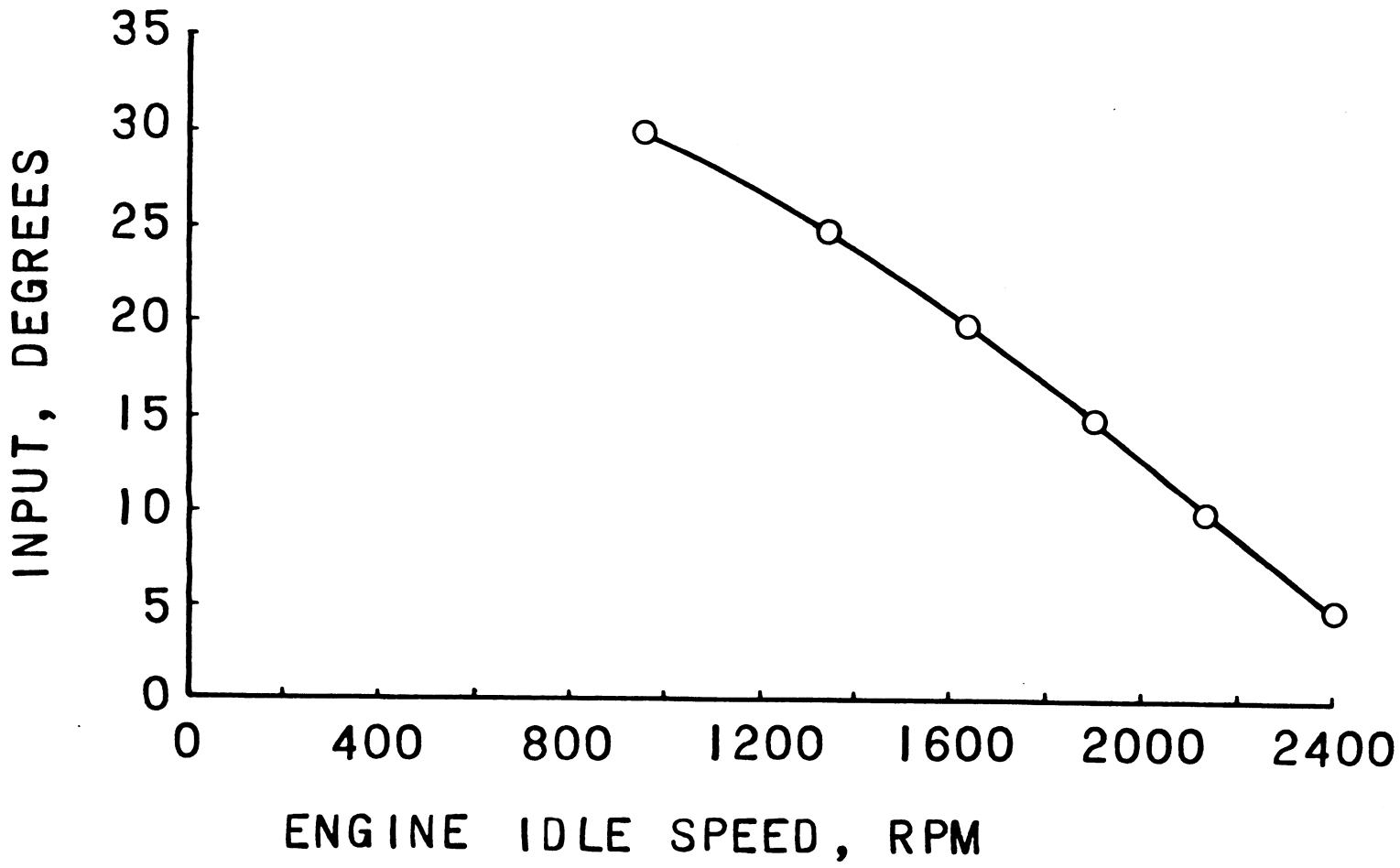

Figure 10. Governor Input Calibration

$$\frac{C_2 C_6 K_1 K_s}{1.1} = \frac{C_6 C_8 \text{ft-lbf}}{1.2 \text{ rpm}}$$

$$K_1 = \frac{1.1\ C_8 \text{ft-lbf}}{1.2\ C_2 K_s \text{ rpm}}$$

$$K_1 = 33.7 \text{ lbm/(hr-lbf)}$$

The remaining parameter C_4 can now be evaluated from Eq. (20).

$$C_4 = \frac{C_8 \text{ft-lbf}}{1.2 \text{ rpm } K_1} - \frac{1}{C_6 K_1} = 0.0022 \text{ lbf/rpm}$$

The dynamometer inertia was found by conducting a frequency response test of the engine connected to the dynamometer to find their combined time constant. From Raven [3] the engine time constant is related to the engine inertia as

$$\tau_2 = C_6 C_8 \frac{2\pi}{60} J_e .$$

When the dynamometer was connected to the engine their combined time constant was

$$(\tau_2 + \tau_d) = C_6 C_8 \frac{2\pi}{60} (J_e + J_d).$$

Solving for $C_6 C_8 2\pi/60$ in both equations and equating the results,

$$\frac{\tau_2}{J_e} = \frac{\tau_2 + \tau_d}{J_e + J_d} .$$

The dynamometer inertia was then calculated by the following equation.

$$J_d = J_e \left(\frac{\tau_2 + \tau_d}{\tau_2} - 1\right)$$

$$= 8.2 \text{ ft-lbf-sec}^2$$

The transmission ratio servomotor time constant, τ_t, was found by a frequency response test with the results shown in Fig. 11.

$$\tau_t = 0.22 \text{ sec}$$

The parameters in Eq. (17) were determined experimentally by applying a sinusoidal input, e_r, with a peak to peak amplitude of 20 volts. The gain $K_l K_{ta} = 0.006$ was evaluated on the asymptote where the frequency was 1 rad/sec. It can be seen from Fig. 12 that the time constant τ_{ta} does not affect the system in the range tested. However, τ_{ta} will not be neglected, but will be kept as a parameter for further study.

An open loop frequency response test was conducted with the governor actuator and the results presented in Fig. 13. The gain constant $K_{gl}K_{ga} = 9.0$ and the time constant $\tau_{ga} = 0.232$.

All the system parameters have been evaluated except for K_g, K_t, and τ_{ta}. The transformed system equations are now written in terms of these parameters.

$$n_p = (1.01\, n_{in} - 1.1\, t_p)/(1 + 0.159\, s) \tag{21}$$

$$n_m = (1450\, r_o + 1.1\, n_p - 1.04\, t_{el})/(1.0055 + 0.866\, s) \tag{22}$$

$$p = 23.9 t_{el} + (0.12 + 20.55\, s) n_m \tag{23}$$

$$t_p = 142\, r_o + 0.046\, p + 0.00615\, n_p \tag{24}$$

$$r_o = r_i/(1 + 0.22\, s) \tag{25}$$

$$r_i = 0.006\, e_t/(1 + \tau_{ta}\, s)s \tag{26}$$

$$e_t = K_t (n_{ms} - n_m) \tag{27}$$

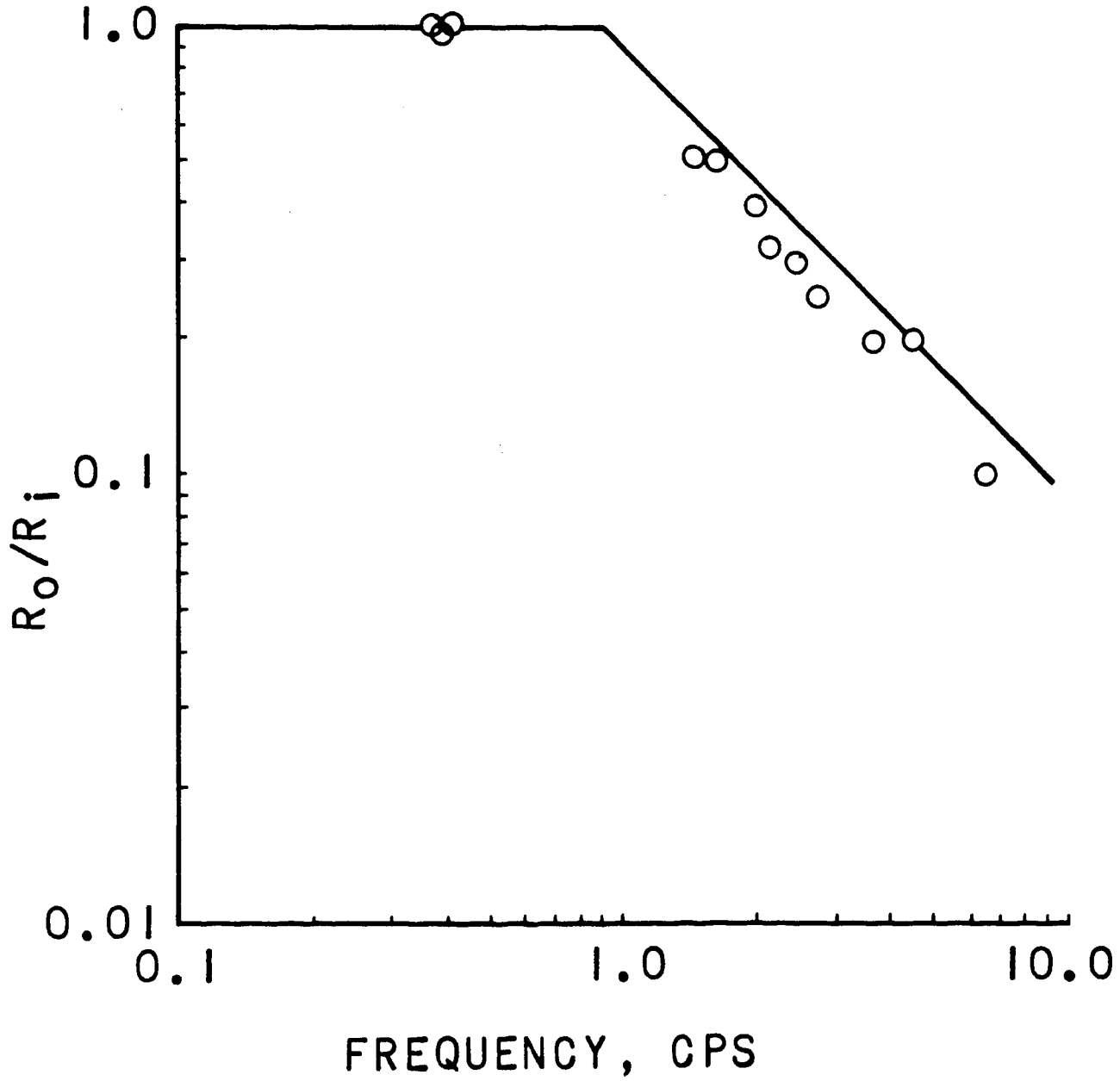

Figure 11. Pump Swashplate Servomotor Time Constant

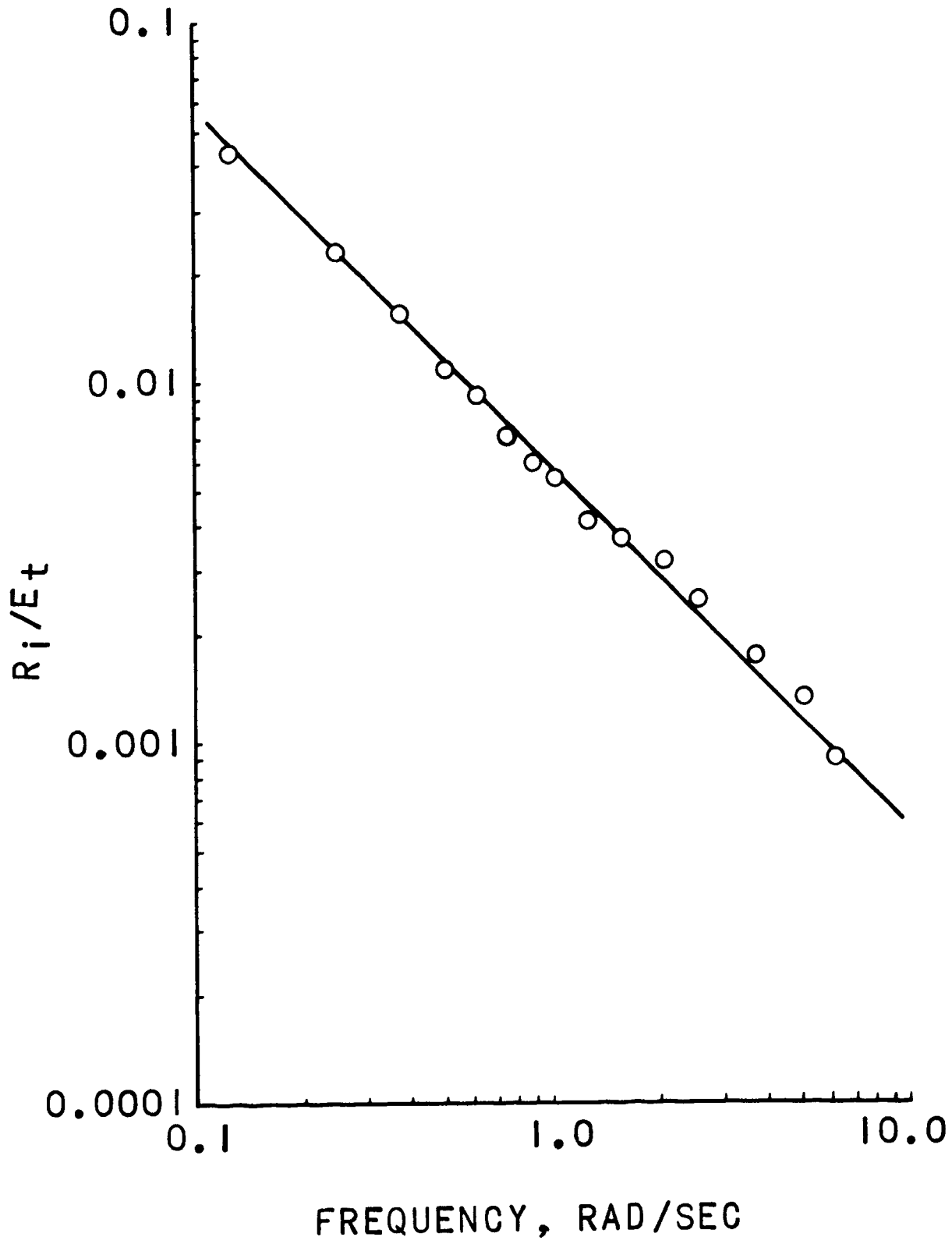

Figure 12. Ratio Actuator Frequency Response

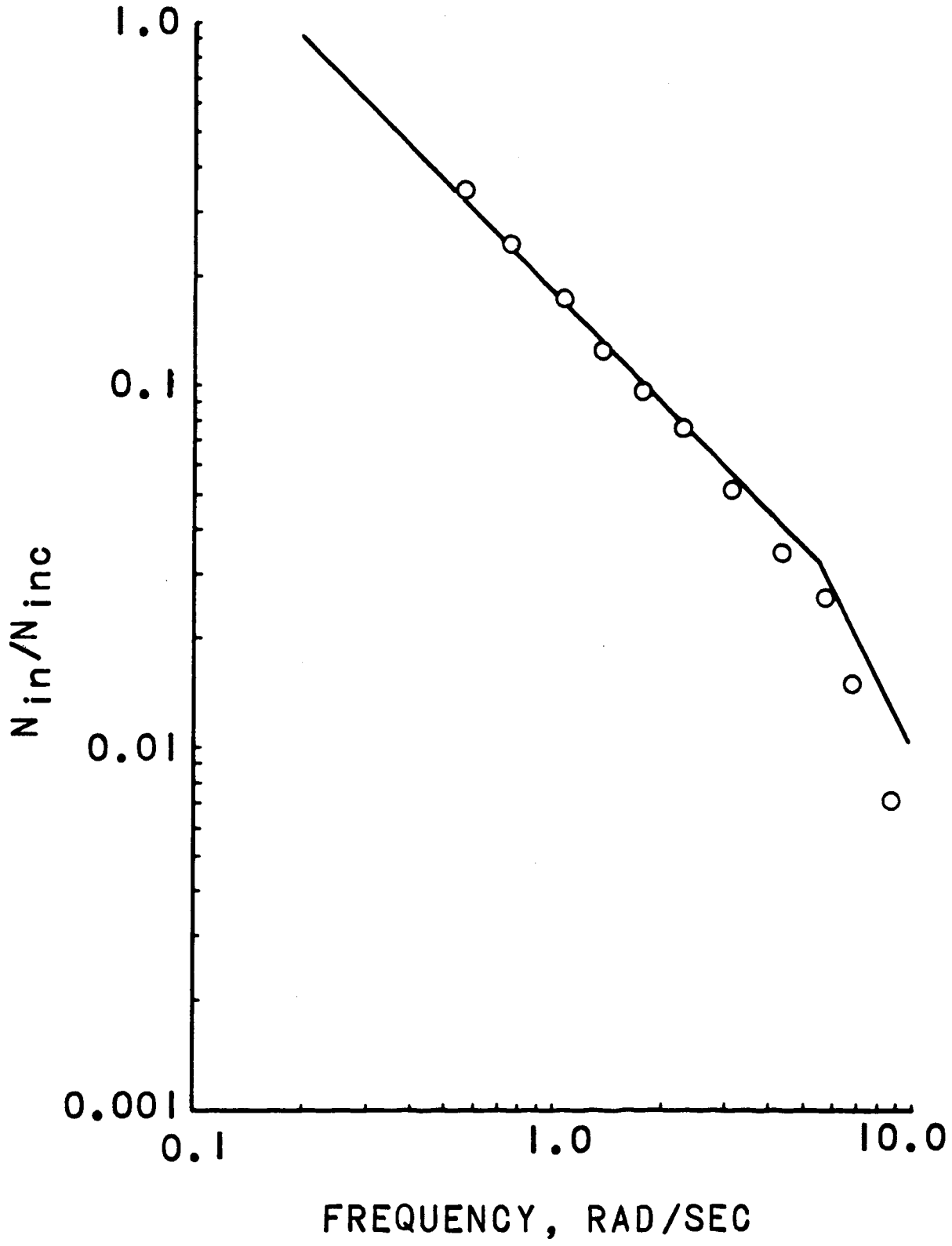

Figure 13. Governor Actuator Open-Loop Frequency Response

$$n_{in} = 9.0\, e_g/(1 + 0.232\, s)s \tag{28}$$

$$e_g = K_g\,(n_{inc} - n_{in}) \tag{29}$$

D. Stability Analysis. It would be impractical to calculate the system response for every possible excitation that could occur, therefore, a general method of determining the basic operation of a system was implemented to evaluate the transient performance of the system. A very good measure of the transient behavior can be obtained from the roots of the characteristic equation. These roots can be presented graphically for study by the root-locus method [3].

The first step in the stability analysis was to obtain the characteristic equation for ratio control only, that is, with the governor control loop open. This was found by substitution from Equations (21) through (27) letting $n_{in} = 0.0$.

$$s\,[0.0302\tau_{ta}s^4 + (0.6155\tau_{ta} + 0.0302)s^3 + (2.39\tau_{ta} + 0.6155)s^2$$

$$+ (1.01168\tau_{ta} + 2.39)s + 1.01168\,]$$

$$+ K_t(1.383s + 7.656) = 0.0 \tag{30}$$

Recalling from Fig. 12 that the time constant τ_{ta} did not influence the system in the region tested, a value was selected for τ_{ta} that was considered to be the extreme case. If $\tau_{ta} \leq 0.2$, its influence would not be seen in the range tested. Figure 14 is the root loci of the system.

The value for K_t must be chosen such that the roots all lie in the left half plane in order for the system to be stable if the governor loop is opened

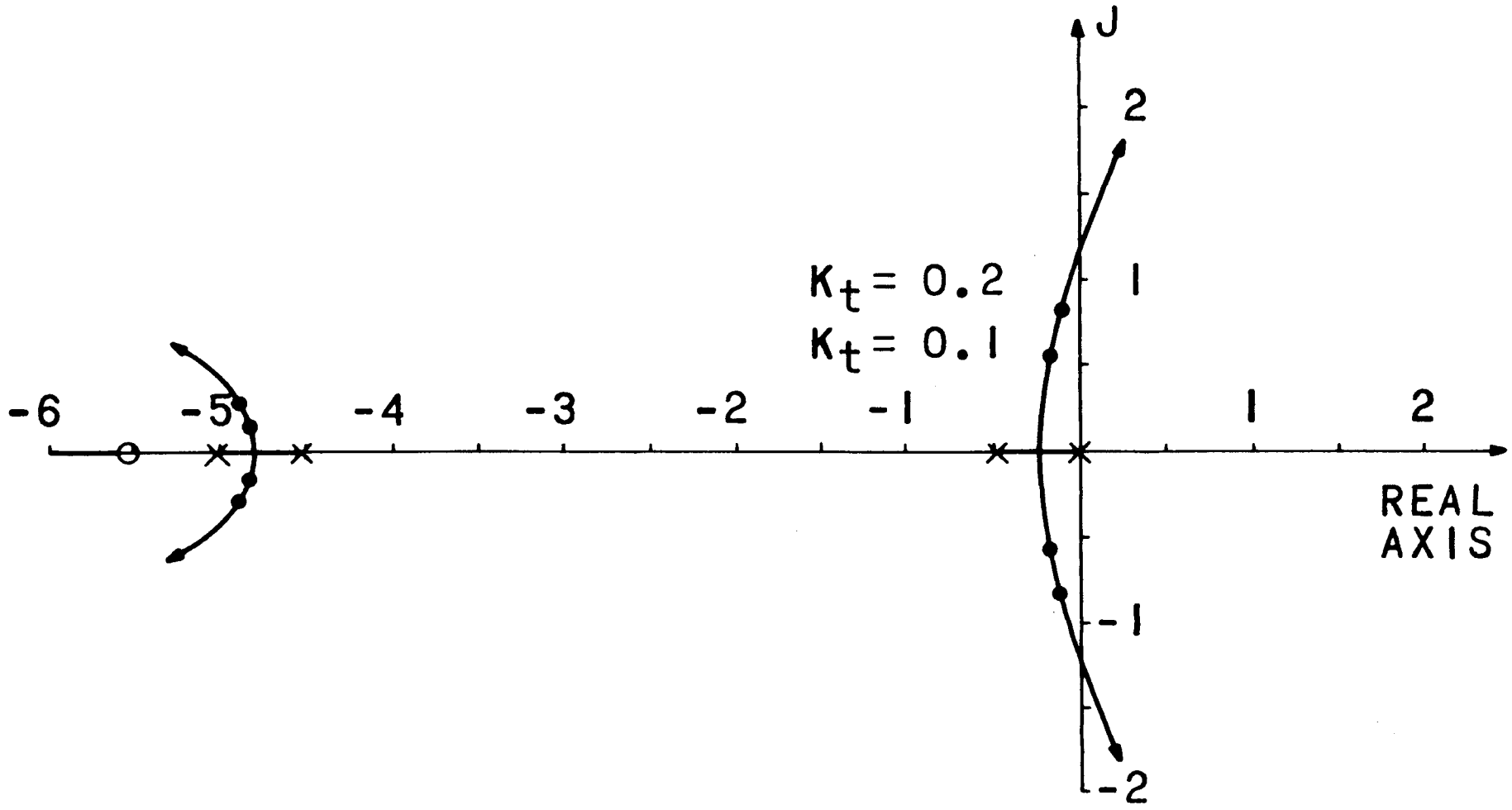

Figure 14. Root Loci for Ratio Control

during operation. From the root locus plot it was seen that the system should be stable for $K_t \leq 0.45$. The damping ratio of a complex root is the cosine of the angle between the root locus vector and the negative real axis. For $K_t = 0.1$ the damping ratio, ζ, of the complex roots nearest the origin was $\zeta = 0.304$ and for $K_t = 0.2$, $\zeta = 0.153$. From graphs [12] of the transient response of a second order system it was seen that $K_t = 0.1$ was more satisfactory because as ζ becomes less than 0.3 the time required for the transients to decay becomes much longer.

The effects of the parameters J_d, J_e, τ_t, and τ_{ta} could then be studied since K_t was fixed. One parameter was varied at a time and the root loci plotted. The first parameter considered was the dynamometer inertia, which was analogus to vehicle inertia. It was important to know how a change in vehicle weight would affect the transient behavior. The root loci was plotted for J_d, $J_d/2$, and $J_d/4$ in Fig. 15(a). It could be seen that as the dynamometer or vehicle inertia was decreased the natural frequency as well as the damping of the system would increase leading to more stable operation. The root loci for J_e, $2J_e$, and $4J_e$ were plotted in Fig. 15(b) and the effect of engine inertia was seen to be generally inverse to the vehicular inertia effect. Therefore, if a change in vehicle weight is anticipated the maximum inertia ratio of J_v/J_e must be used for the design specifications as this represents the most critical condition.

The effects of changing the time constants of the servomotor and the actuator motor are shown in Fig. 16(a) and Fig. 16(b) respectively. In both

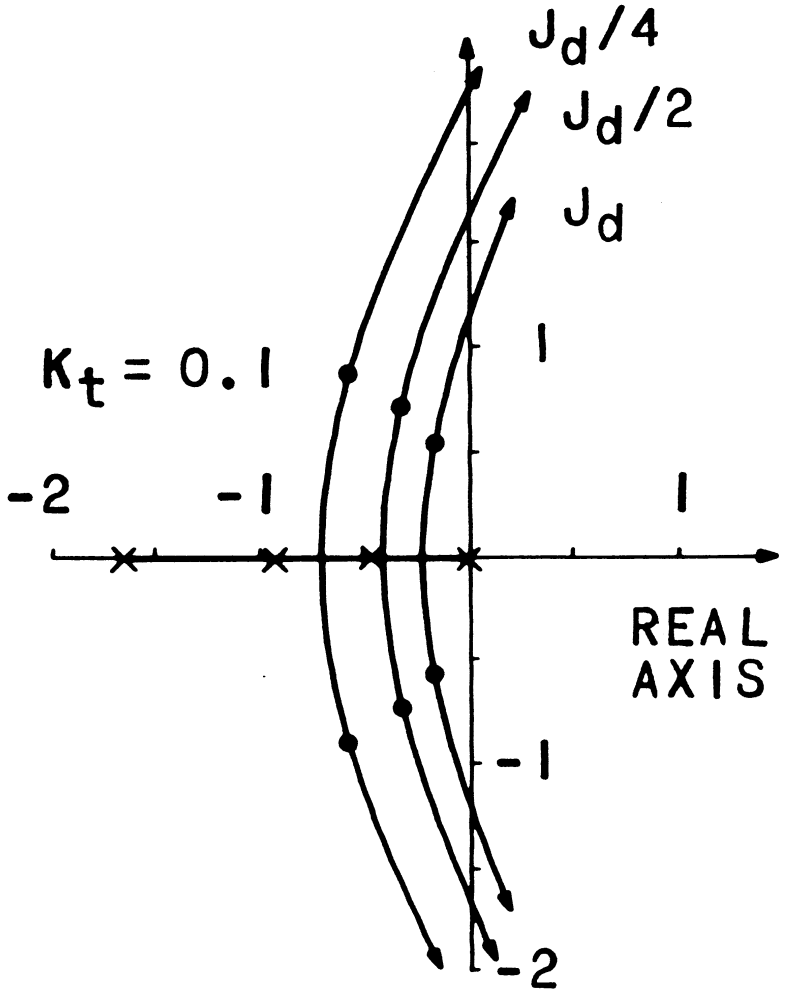

(a)

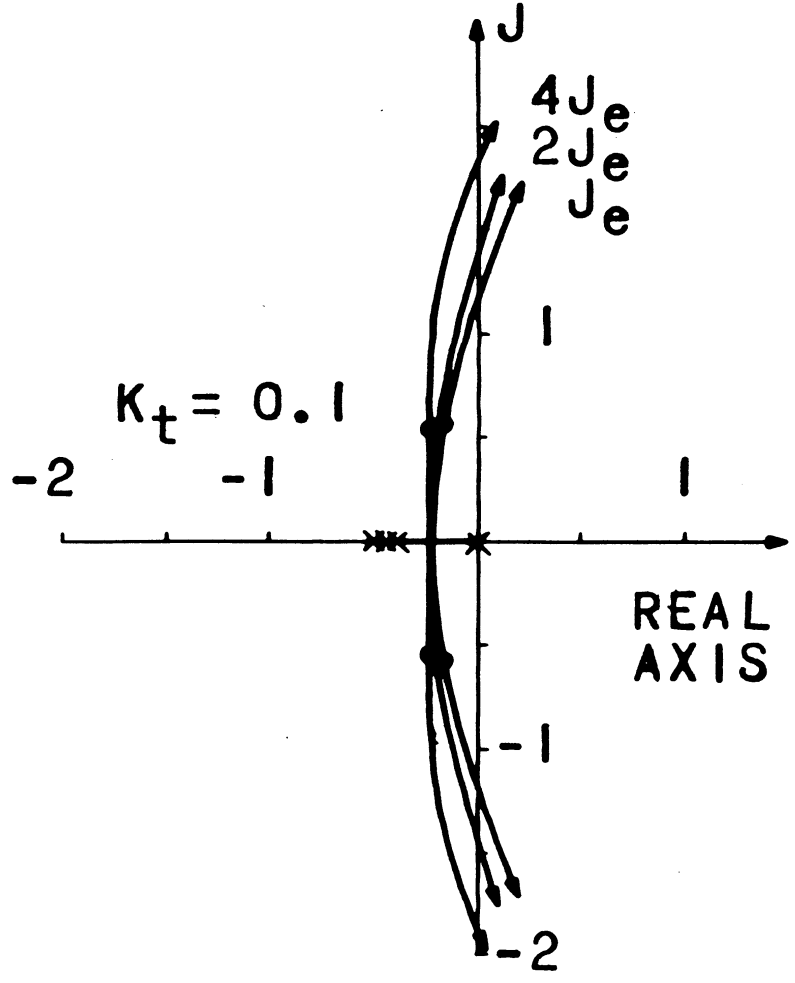

(b)

Figure 15. (a) Dynamometer Inertia Effects; (b) Engine Inertia Effects

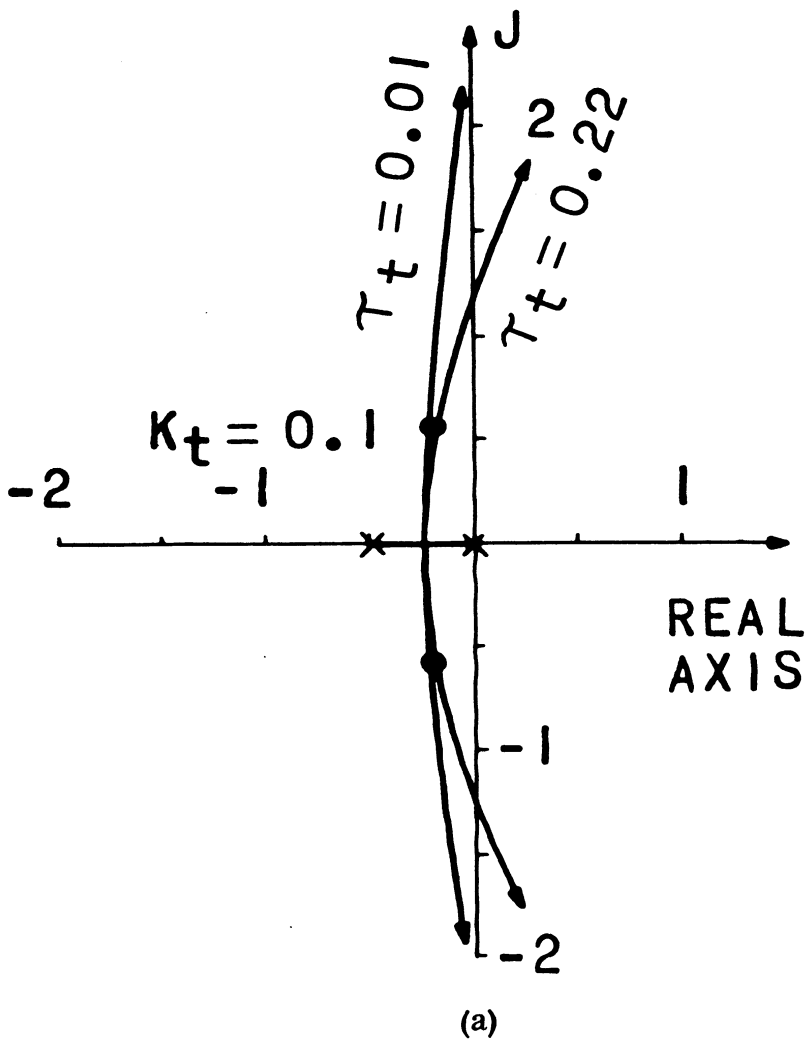

(a)

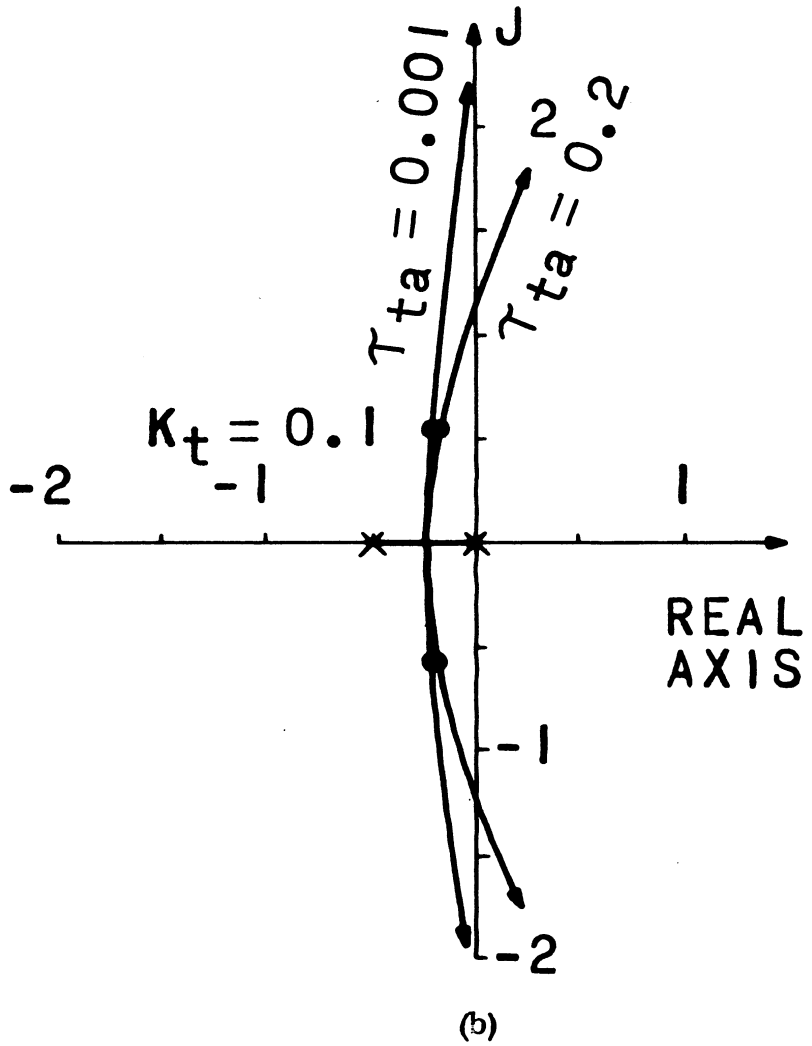

(b)

Figure 16. (a) Ratio Servomotor Time Constant Effects; (b) Ratio Actuator Time Constant Effects

cases the time constants were reduced to produce faster time response. For a large change in either time constant the root locus was changed only slightly at $K_t = 0.1$. The effect of reducing both time constants was plotted in Fig. 17. This would approximate the characteristics of an electro-hydraulic servo-valve supplying oil to the swashplate pistons. This would typically be the final control element needed in any industrial application.

The governor control loop was then closed and the characteristic equation in terms of the parameters K_p and K_g was

$$[s^7 + 29.45s^6 + (292.5 + 38.8K_g)s^5 + (1205 + 985K_g)s^4 + (2040 + 7000K_g)s^3 + (942 + 16,600K_g)s^2 + (545 + 7350K_g)s + 4900] - 296.5K_gK_p[s^4 + 9.57s^3 + 22.85s^2 + 0.267s - 1.92] = 0.0. \quad (31)$$

It was noted here that the gain in Eq. (31) was negative indicating the root loci of interest for this equation was the 0^o phase loci instead of the 180^o phase loci plotted when the gain is positive. This is a result of the positive feedback mentioned earlier.

A linear curve was drawn through the minimum BSFC points in Fig. 5. The inverse of the slope of this line was $K_p = 38$. An arbitrary value was then selected for K_g as 4 volts per 100 rpm. This value was chosen because the governor controller exhibited a dead band characteristic of about 4 volts, therefore, with $K_g = 0.04$ the engine speed input should be within 100 rpm of the calculated value. The root loci of Eq. (31) was then plotted in Fig. 18 with $K_g = 0.04$. A pair of roots entered the right half plane, indicating unstable

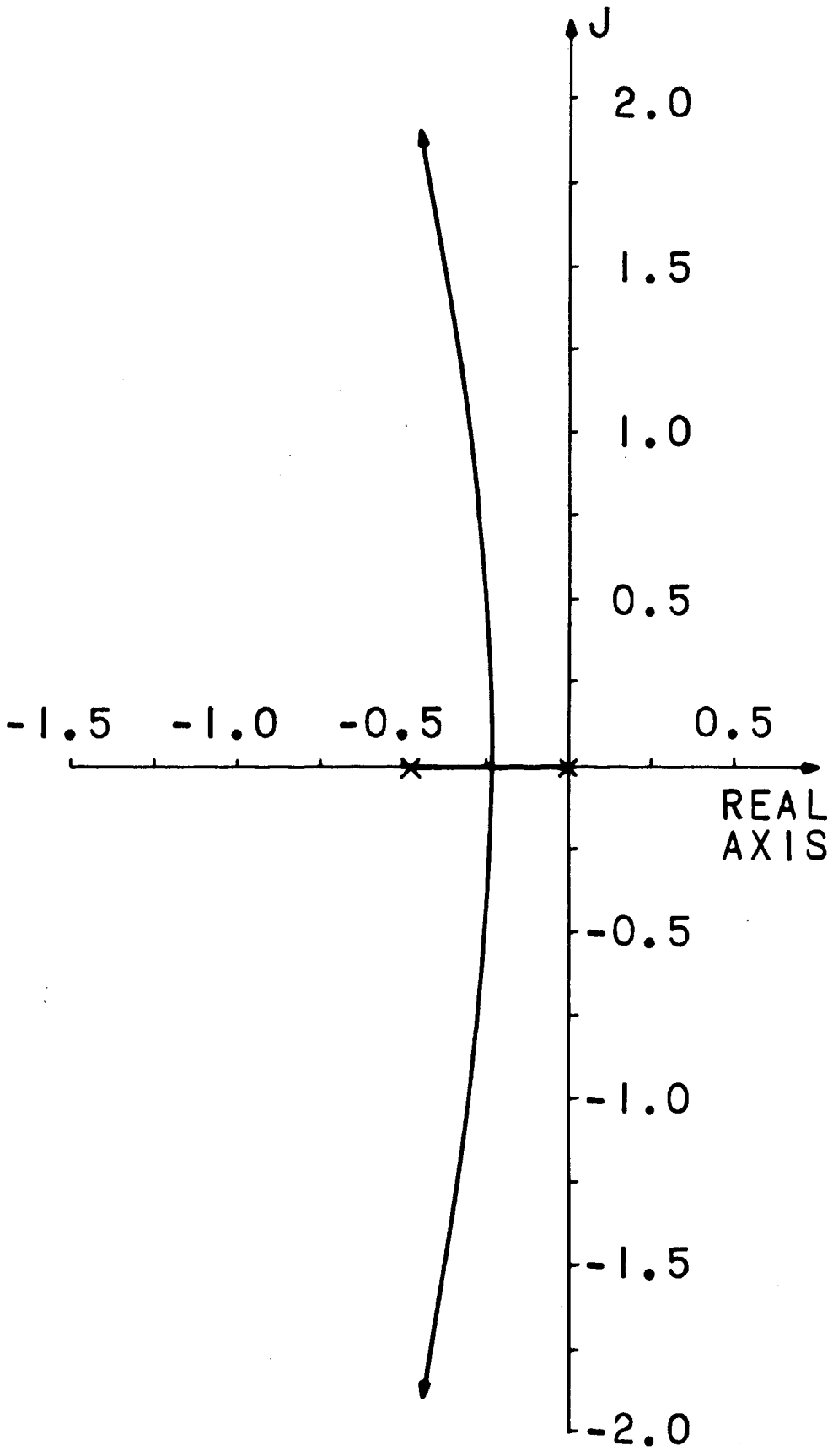

Figure 17. Root Locus With Electro-Hydraulic Servo-Valve

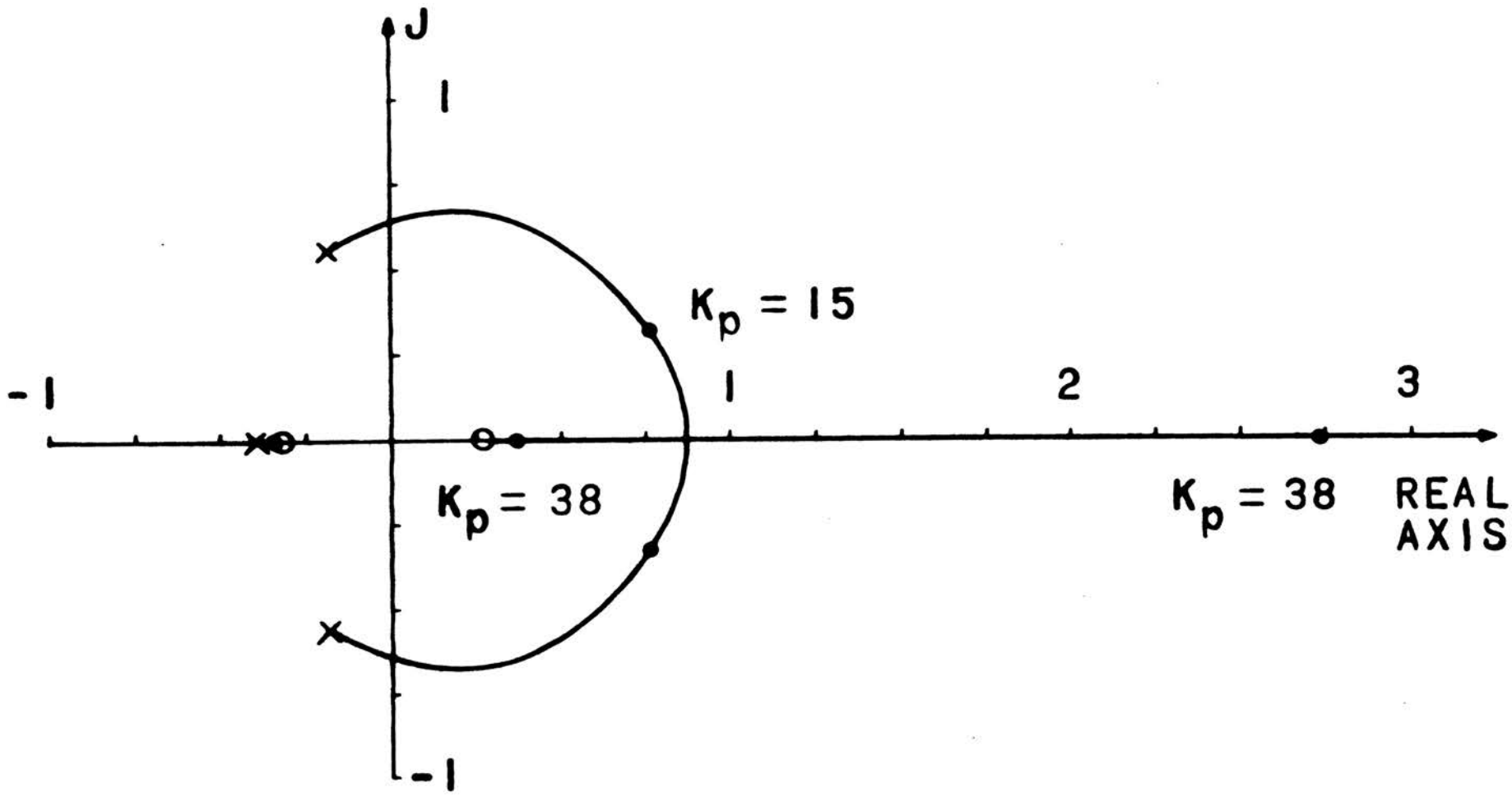

Figure 18. Root Loci for Ratio and Governor Control

operation, at K_p approximately equal to 2.0.

Since there was so great a difference between the design value of K_p and the value for which the system would be stable, it was considered wise to investigate the loss in steady-state efficiency if K_p was decreased.

Figure 19 shows the minimum BSFC curve and also curves of the minimum BSFC plus 2%. Therefore, along a straight line drawn through this region the BSFC was never more than 2% greater than the minimum. A line with slope of 1/15 was drawn through this region and the root locus when $K_p = 15$ was plotted on the curve in Fig. 18.

A pair of roots still existed in the right half plane after the gain constant K_p was reduced to within acceptable steady-state error specifications. To achieve stability it was necessary to design a compensator to force the roots of the characteristic equation into the left half plane.

Compensator design techniques have been developed by Ross, Warren, and Thaler [13] and Hsu [14]. Using these techniques a root can be forced to a certain position in the s-plane. If this new position lies in a phase loci region of $(0^{\circ}$ to $180^{\circ}) \pm k360^{\circ}$, lag-lead compensation is needed and the region $(-180^{\circ}$ to $0^{\circ}) \pm k360^{\circ}$ requires lead-lag compensation. In this case the frequency of the roots could be increased with lead-lag compensation, however, the compensator amplifies the noise generated by the system and feedback transducers and produces unacceptable results.

The new position was located in the lag-lead compensation region at the same angle as the poles to provide the same damping coefficient. Also the

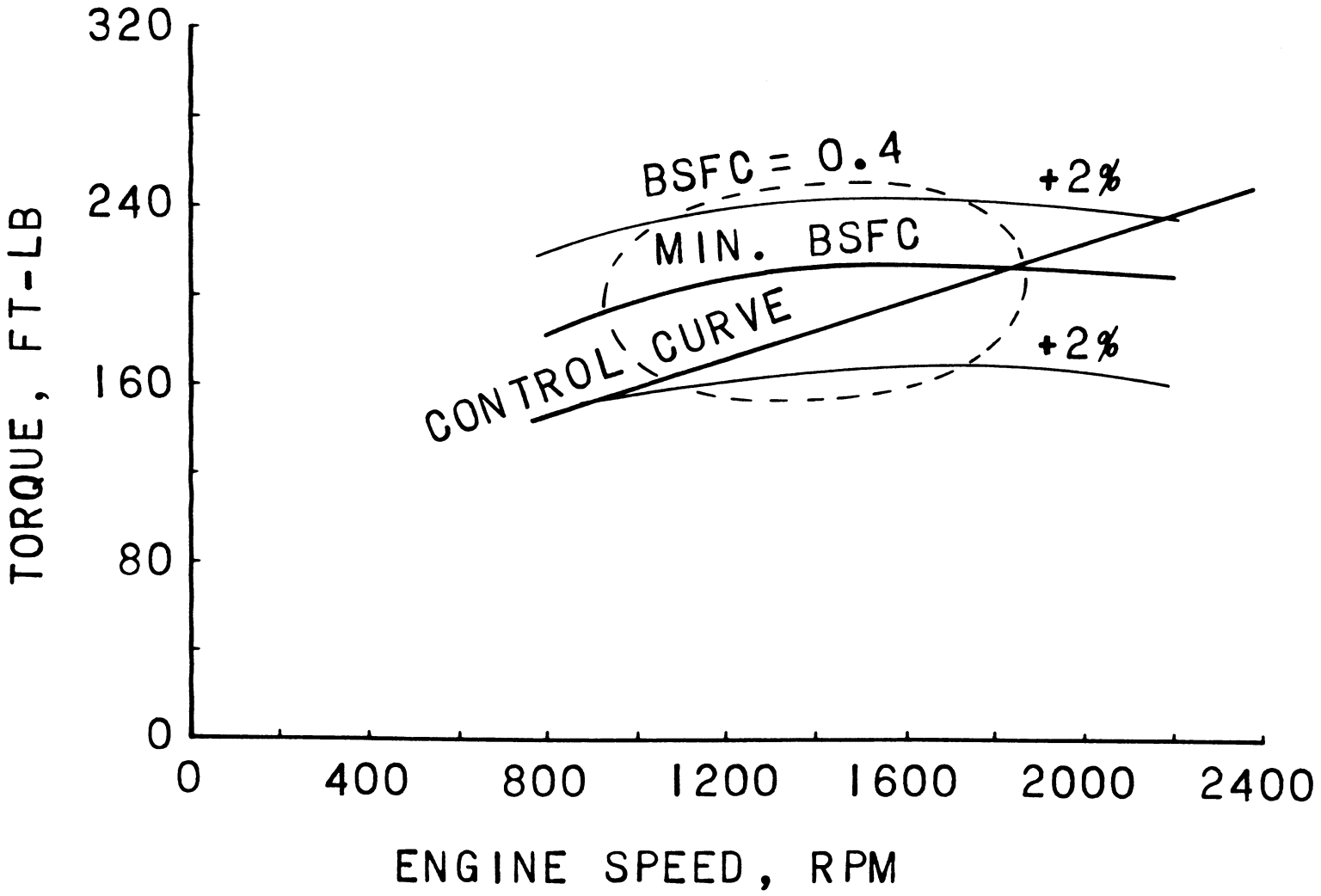

Figure 19. Approximation to the Optimum Curve

design point was placed close to the poles to minimize the loss in frequency of the response. Applying the method of Hsu at the point -0.175 + j0.525 a compensator design of the form

$$G_c(s) = \frac{(1 + \tau_z s)^2}{(1 + \tau_p s)^2}$$

was found. After the compensator parameters were determined it was necessary to plot the loci of the other roots of the system to check their positions. Although the new positions of one pair of poles are specified another pair may have been driven into the right half plane. The partial root loci of the compensated system terminating at $K_p = 15$ was plotted in Fig. 20. The movement of the high frequency roots as K_p increased were attenuated by the lag-lead compensator, hence, only the low frequency root' s movements were important to this investigation.

E. Experimental Tests. The engine and transmission components used in the tests were a 92 horsepower John Deere "4020" diesel tractor engine Serial No. 23F83273, a Sunstrand variable displacement hydraulic pump Model No. 22-2046, and a Sunstrand hydraulic motor Model No. 21-3023. The governor actuator was a modified Airborne Accessories Corp. linear actuator Model R5210M3-4, and the ratio actuator was a modified Airsearch Mfr. Co. actuator Model 25040. The controller was patched on a Heathkit Model ES-400 analog computer and the compensator was patched on a Heathkit Model EC-1 analog computer. The current gain for the governor actuator was a Hewlett-Packard Harrison 6824A Power Supply Amplifier and for the ratio actuator a

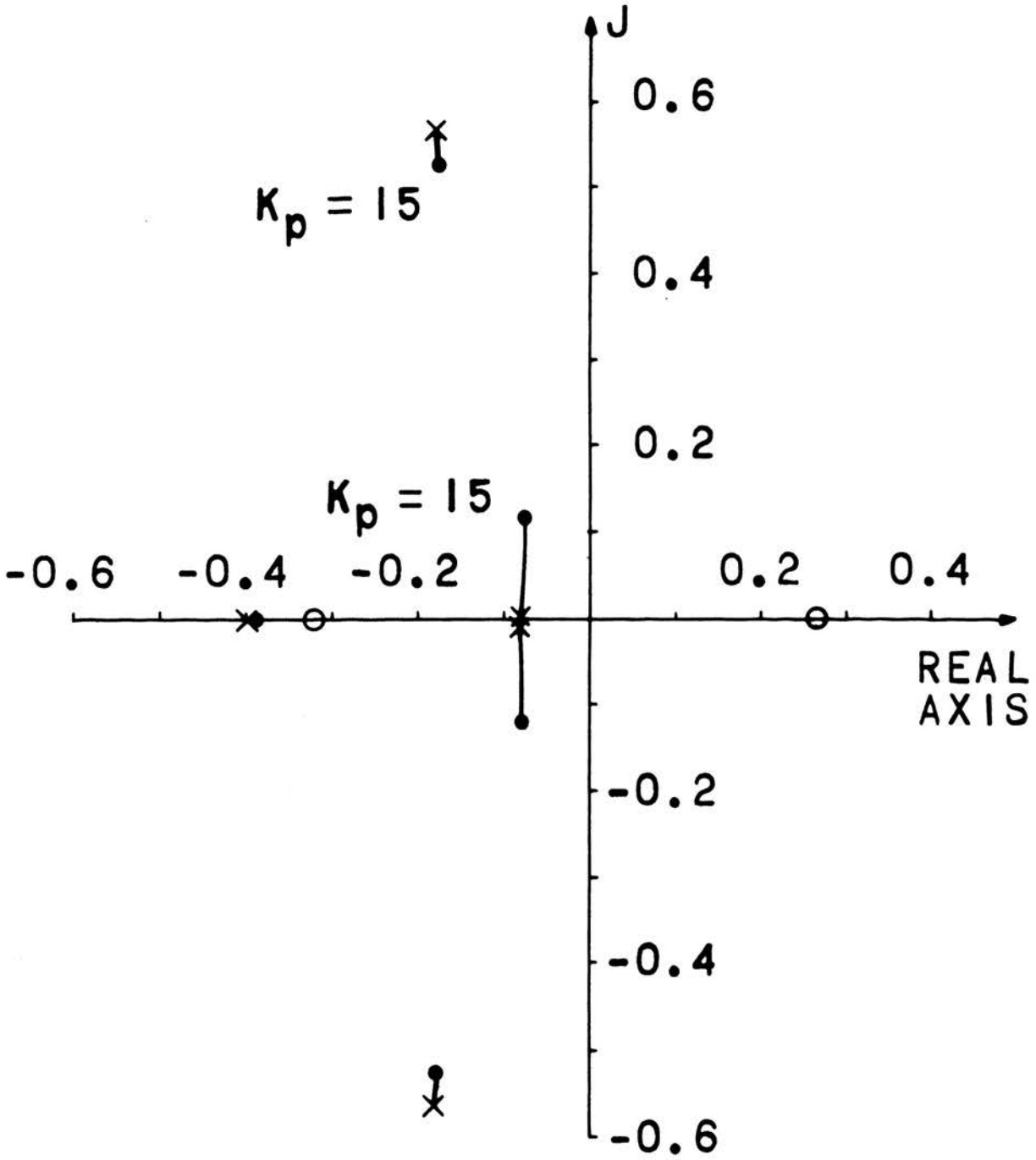

Figure 20. Compensated System Partial Root Loci

current gain device was constructed by the author. The Appendix contains more detailed information on these electronic sub-systems.

The engine and transmission were connected to a General Electric dynamometer No. 1757633, capable of absorbing up to 100 horsepower, located in the Mechanical Engineering Systems Laboratory at the University of Missouri - Rolla. The dynamometer controls were developed by M. E. Downs [15] to maintain constant torque by varying the field current under changing speed conditions. A schematic of the system is given in Fig. 21.

The ratio control loop was closed and the engine and transmission were allowed to warm up for about fifteen minutes until the engine and transmission temperatures reached steady-state. The engine idle speed was set at 1600 rpm, the transmission output speed was brought to zero, and the ratio controller gain set at $K_t = 0.1$. The input speed setting N_{ms} was then given a step input of 1450 rpm and the output speed response recorded. After steady-state conditions were established, N_{ms} was decreased to check the response at a different level. The procedure was repeated to $K_t = 0.2$ and $K_t = 0.3$. The results are shown in Fig. 22.

The engine and transmission were then set to the specified reference conditions and the control loop for the governor actuator was closed and the reference torque given a -20% step change. The resulting transient response is shown in Fig. 23. It was observed that the actuators were both reaching their travel limits, therefore, the amplitude of oscillation was limited by the physical constraints after about 1.5 cycles of operation.

The system was again brought to the reference conditions and the

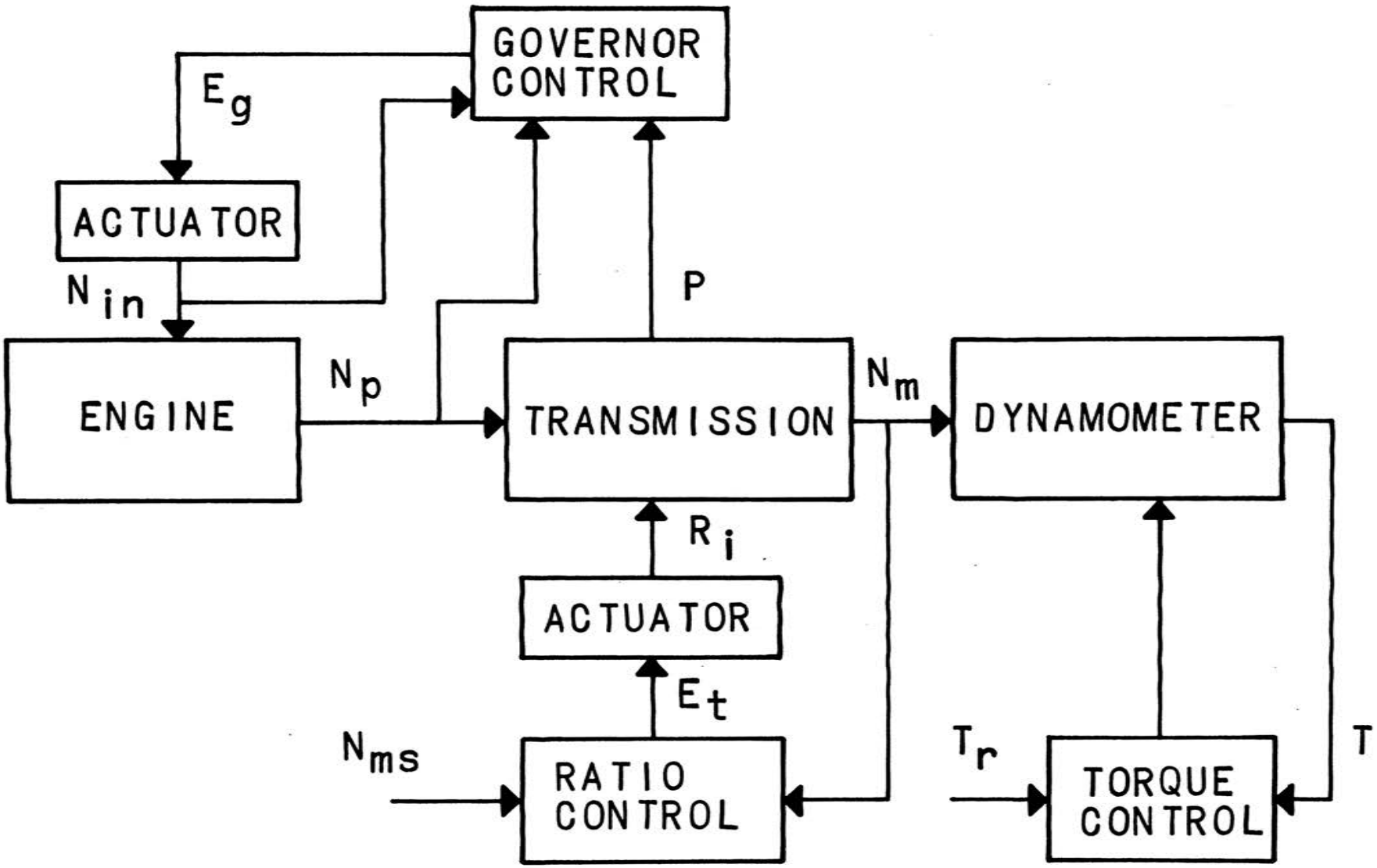

Figure 21. System Block Diagram

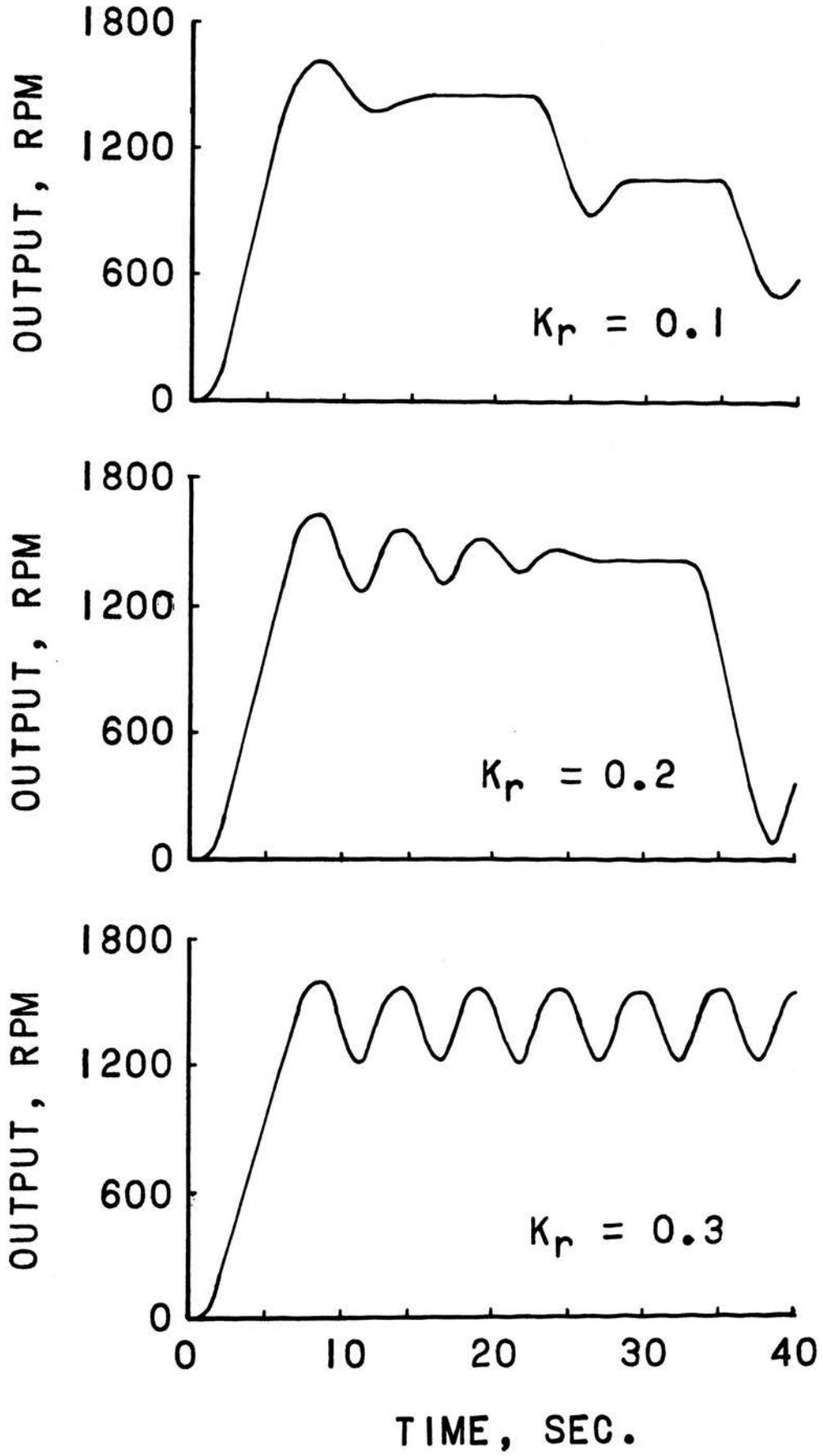

Figure 22. Response of Ratio Controlled System

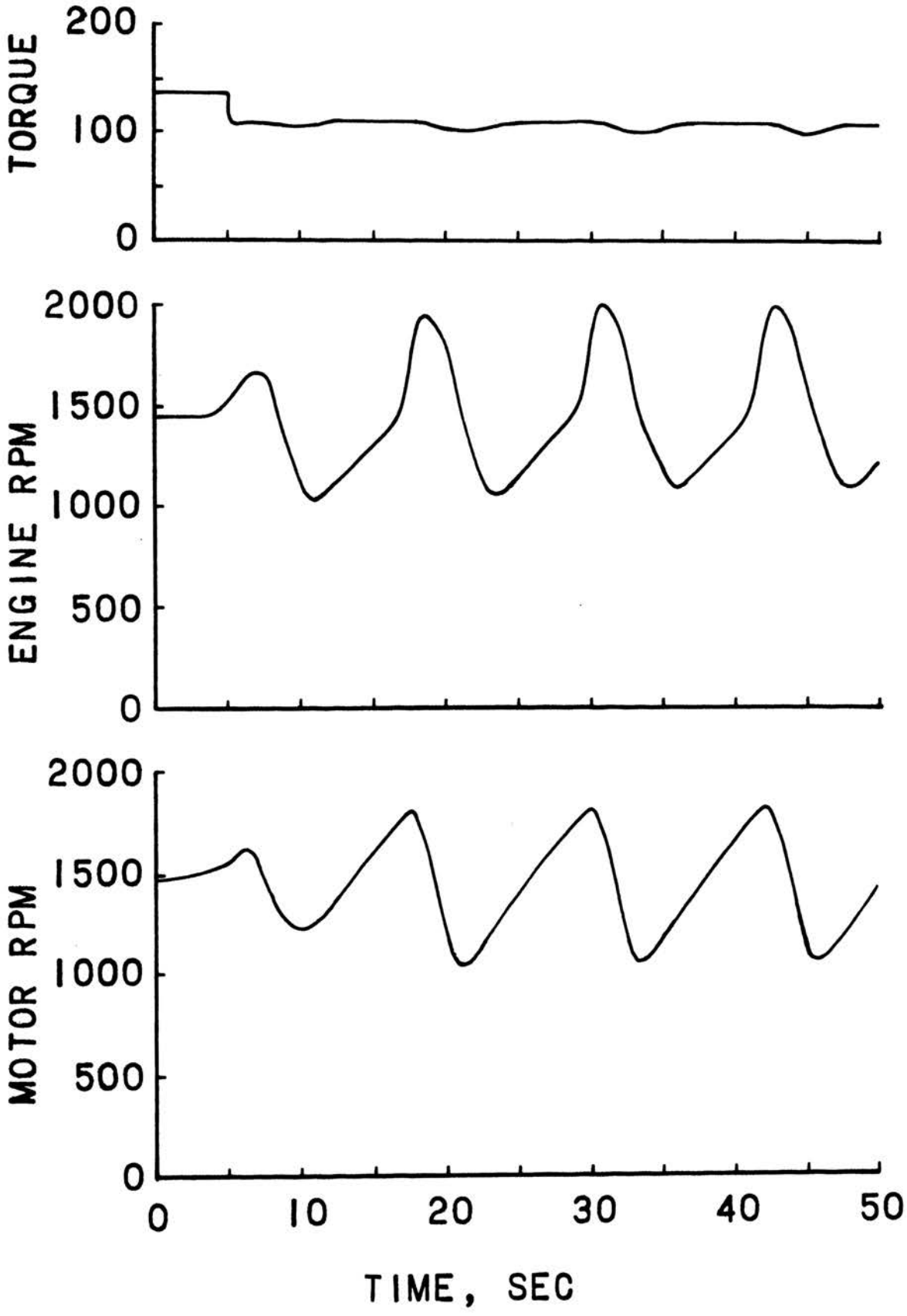

Figure 23. Response of Uncompensated System

compensator patched into the control circuit. Again the governor control loop was closed and the reference torque given a -20% step change. After the transients decayed and steady-state conditions were established, the step input was removed and the system response plotted in Fig. 24 and Fig. 25 respectively. The same procedure was followed for a +20% step and the system response presented in Figures 26 and 27.

F. Discussion of Results. The mathematical model is an approximation to the physical system. Before the model can be used for design purposes there must be evidence to establish a confidence level in the system representation. Two types of tests were conducted and from these experiments the accuracy of the model was estimated.

The data plotted in Fig. 22 from the transient response of the ratio controlled system was presented in root locus form in Fig. 28 for comparison to the theoretical root locus. The experimental tests indicated higher frequencies and lower damping ratios than those predicted theoretically. For $K_t = 0.1$ the frequency and damping ratio were 31.5% higher and 22.5% lower, respectively, than the theoretical values. For $K_t = 0.2$ the experimental frequency and damping ratio were 34% higher and 47.5% lower, respectively, than the predicted values. It was considered that the data for $K_t = 0.3$ should not be used for comparison as the system was obviously saturated during this portion of the response. Returning attention to the experimental points plotted in Fig. 28, it was noticed that the experimental point for $K_t = 0.1$ was close to the theoretical curve for K_t approximately equal to 1.5. If the gain in the model was increased, the representation would be closer, however, since

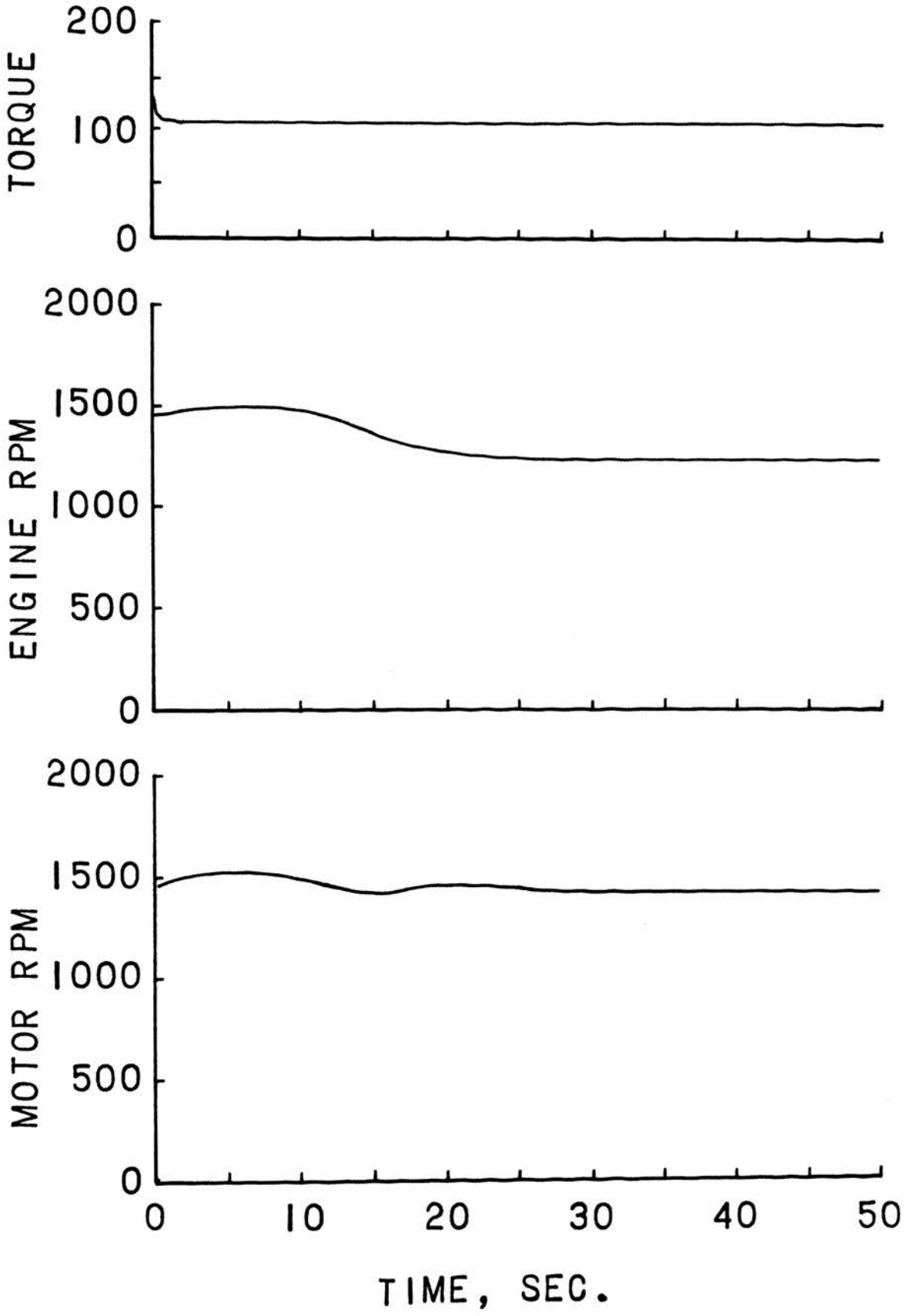

Figure 24. Response to -20% Torque Step

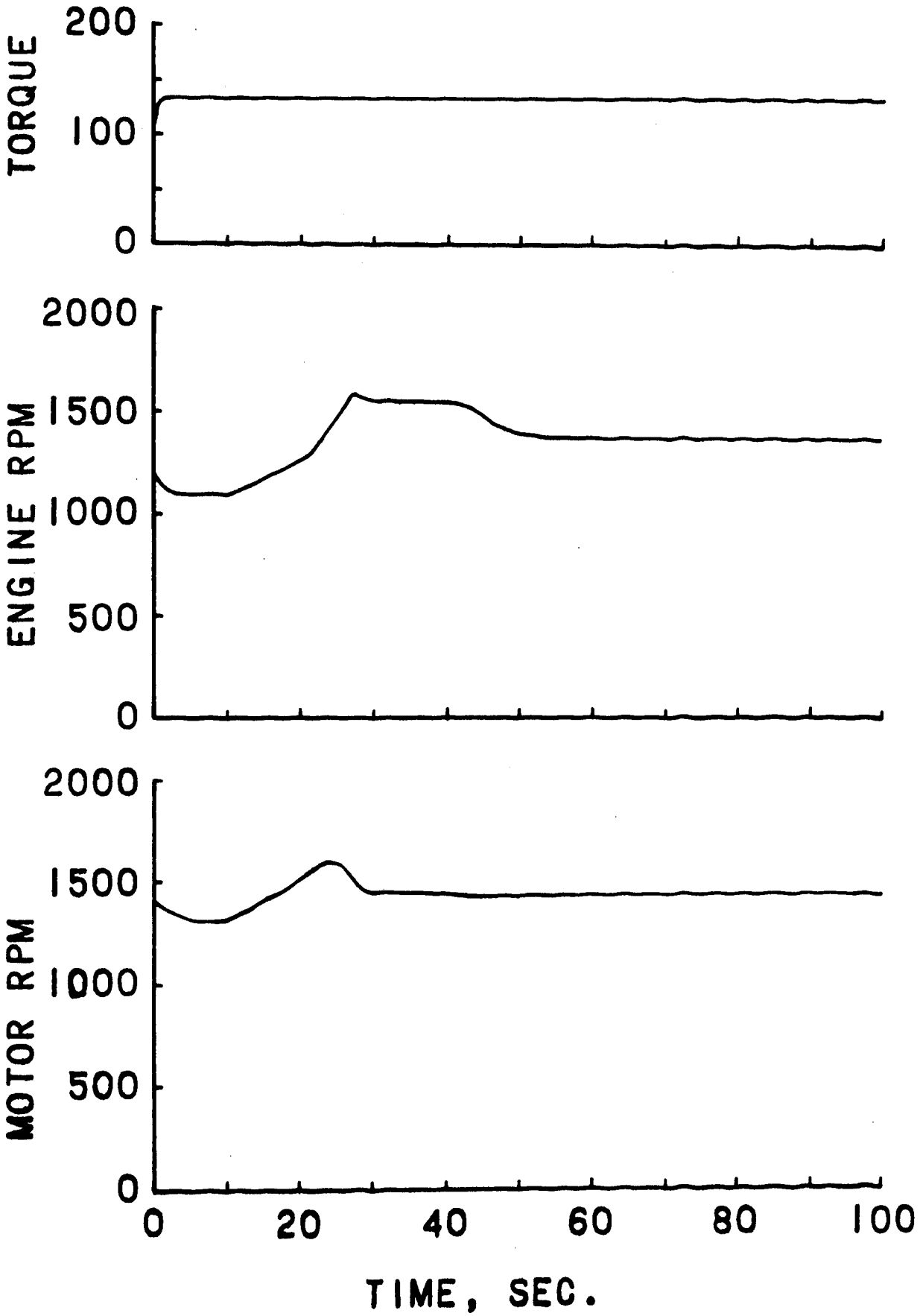

Figure 25. Response to Removal of -20% Torque Step

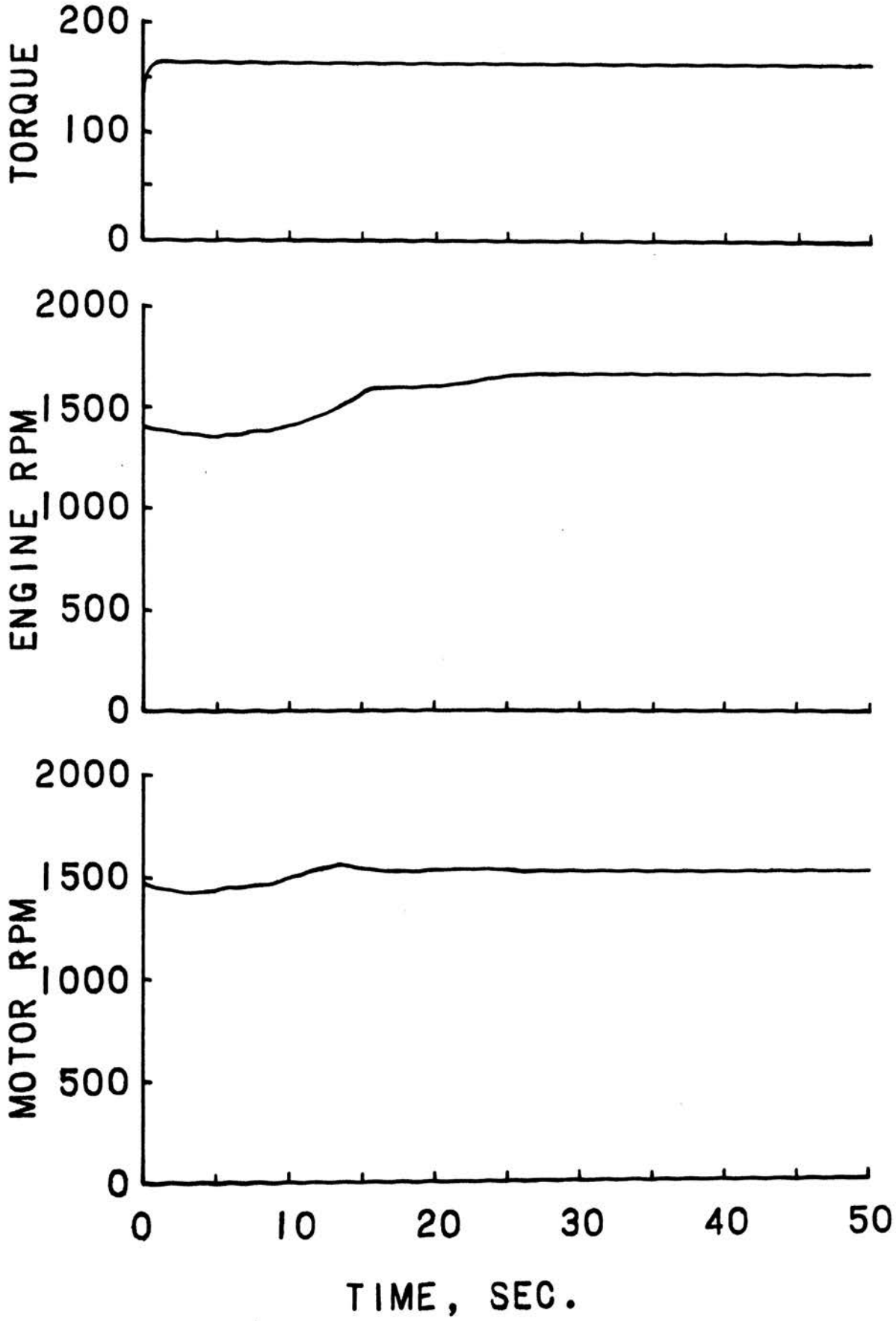

Figure 26. Response to +20% Torque Step

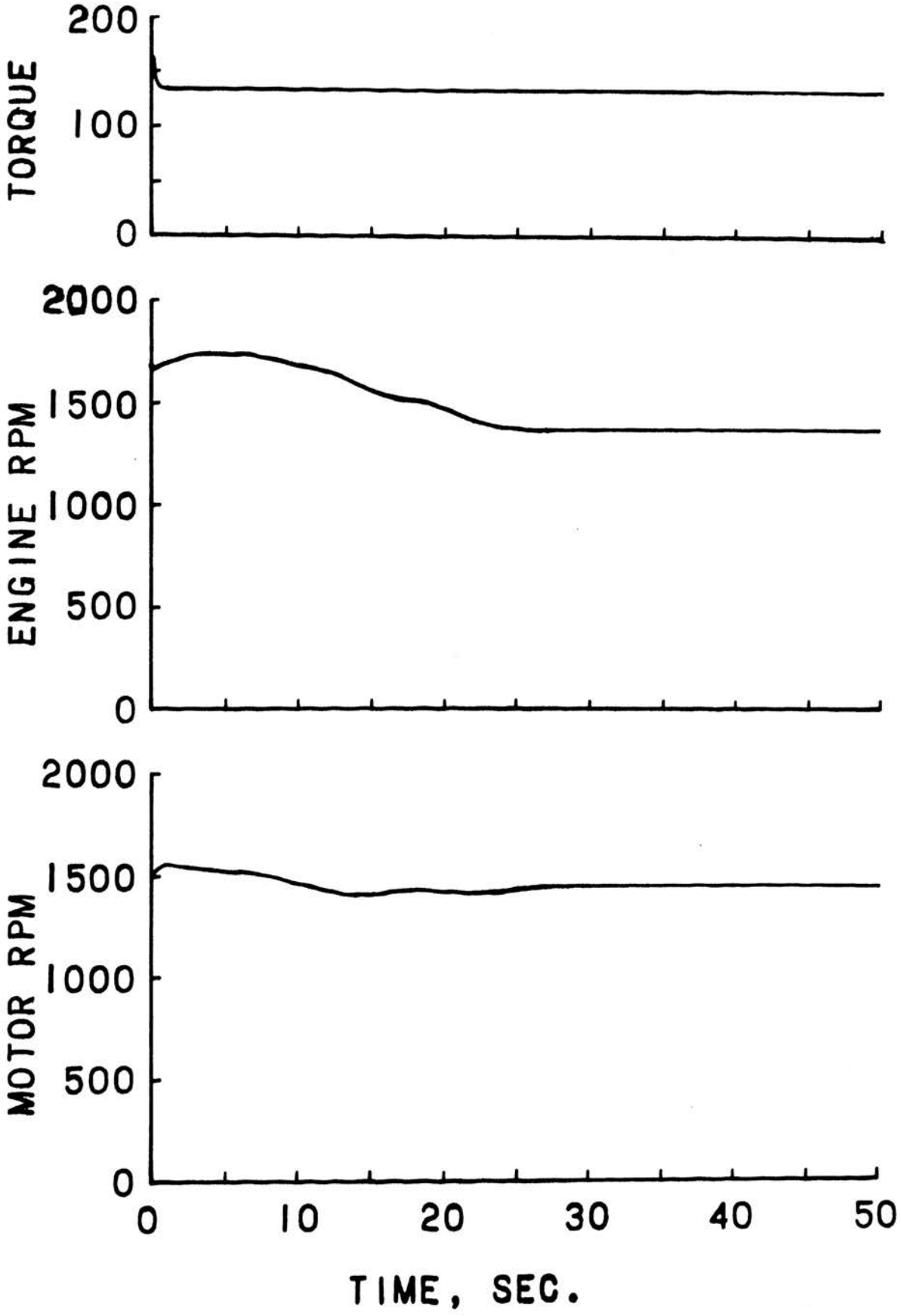

Figure 27. Response to Removal of +20% Torque Step

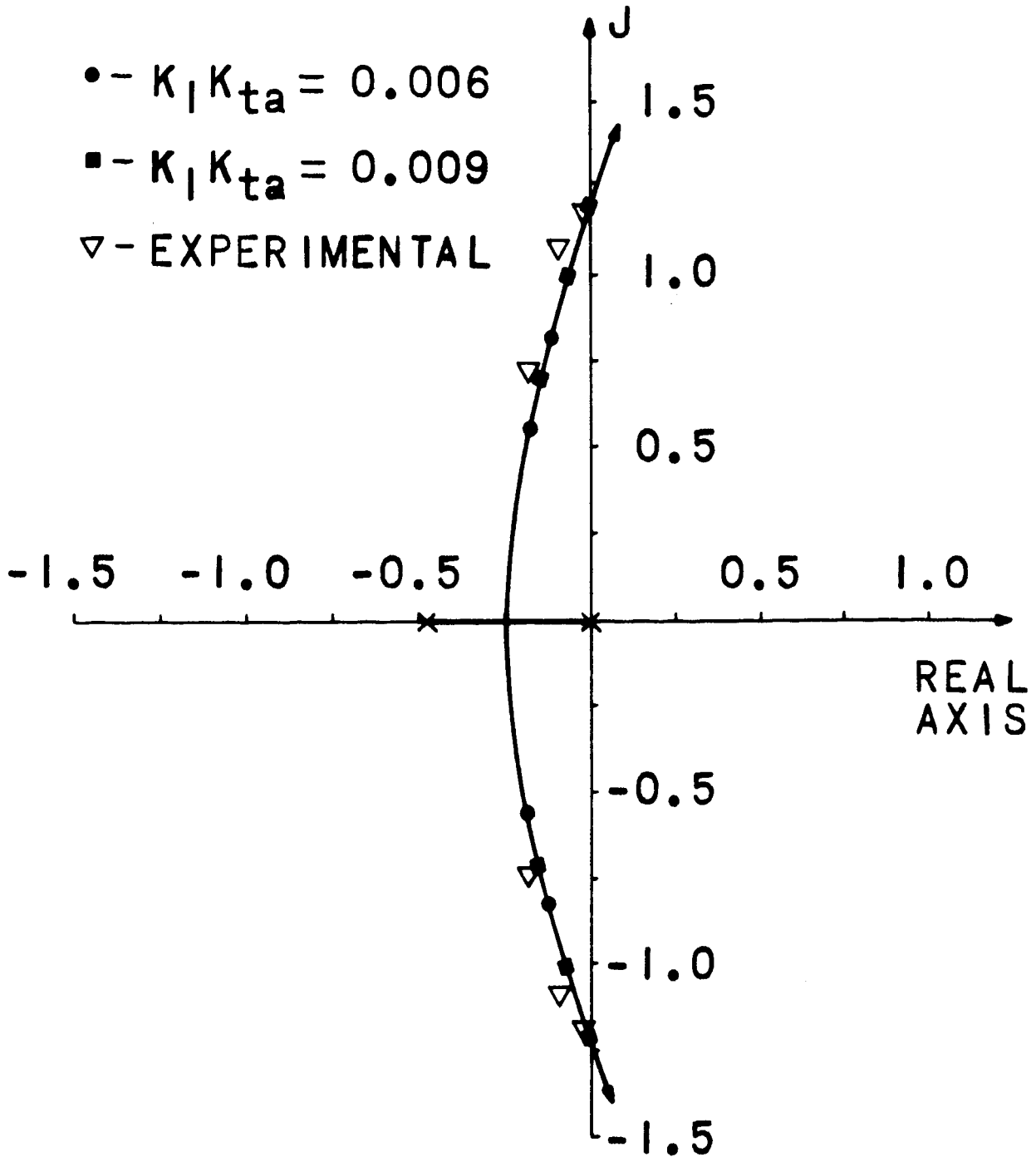

Figure 28. Ratio Control Experimental Results

K_t was a gain setting on the controller it was best to change K_1K_{ta} as K_t and K_1K_{ta} appear as a product in Eq. (17). The theoretical points for $K_1K_{ta} = 0.009$ were plotted in Fig. 28 where a much closer correspondence to the experimental data can be seen.

An examination of the system response of Fig. 23 revealed the response was indeed unstable increasing in amplitude until bounded by the limitations of the system. Neither the response of the motor or the engine was sinusoidal, but both were periodic with frequency of 0.513 rad/sec. Because of the fact that most of the subsystems, the ratio controller, governor controller, and swashplate servomotor, were saturated during part of each cycle very little comparison could be drawn with the model except that the predicted instability was present.

The compensated system response was stable and the time for the engine and motor speed to reach steady-state was approximately 27 sec. in each case except for the test shown in Fig. 25. When the -20% step was removed the engine transients did not decay to acceptable levels until 54-56 sec. This test was conducted more than once with the results being identical each time. No explanation was found as to why this response should be different than that for the addition of a 20% step to the reference torque (Fig. 26). This test shown in Fig. 25 was the only one which had overshoot in the engine speed. It can be seen in Fig. 24 and Fig. 27 that the subtraction of a 20% torque step produces the same form of response irrespective of the initial value. The engine speed momentarily increased due to the lower torque level, then decreased until reaching the steady-state value after about 27 seconds.

This time was one half of the time required for the engine to reach steady-state after the overshoot in Fig. 25.

Looking at the characteristic equation with $K_1K_{ta} = 0.009$ the damped natural frequencies of the two pairs of complex roots nearest the origin were 0.0955 rad/sec. and 0.659 rad/sec. corresponding to the compensator and the ratio controlled system respectively. The system's dynamic behavior should be the sum of the contributions of all its roots with the predominant effects coming from the two pairs of complex roots just mentioned. The highest discernable frequency present in the motor speed response was most easily measured in Figures 24 and 27 and in both instances was approximately 0.628 rad/sec. The lower frequency was 0.116 rad/sec., if one can assume the 54 sec. in Fig. 25 were one complete cycle and the 27 sec. in Figures 24, 25, and 27 were one half cycle. The deviation was 22% with the lowest frequency and 4.5% with the higher frequency.

The steady-state error in the output speed was a maximum +73 rpm and -37 rpm when approaching the reference value from above and below, respectively. This indicated a dead-band of 100 rpm or ±5 volts in the ratio control system. This error was 6.9% at the reference speed, however, at very low speeds this error would be intolerable. For a controller to function satisfactorily at low speeds the dead-band must be reduced to a very low value. One method of reducing the dead-band, and the two time constants τ_{ta} and τ_t also, would be by employing an electro-hydraulic servo-valve in place of the swashplate servomotor and the electric linear actuator.

The dead-band on the governor control was 100 rpm, hence, as a

proportional position controller the dead-band could add on both ends giving a maximum error of 200 rpm. In Fig. 23 the steady-state error in the engine speed was 182 rpm. This would not affect efficiency much at the lower end of the minimum BSFC curve, perhaps 2-4%, because the constant horsepower lines are curving in the same direction as the lines of constant BSFC. But at the high end of the minimum curve the curvature is opposite and this could cause as much as 10% error in efficiency. The gain K_g could be increased lessening the amount of dead-band in the engine speed. This would in turn require the compensator to be slower to maintain system stability.

After the correlation between the model and the physical system was established, the model was extended to investigate the design of a control system for a representative vehicle. First the torque term due to inertia was changed to represent the translational inertia of a 10,000 lb. vehicle moving at 5 mph. Then the governor controller gain was increased to $K_g = 0.06$ to lower the dead-band to ±67 rpm. The time constants τ_{ta} and τ_t were reduced to 0.001 sec. each and the gain K_t increased to 0.5 from 0.1 to approximate an electro-hydraulic servo-valve supplying the oil to move the swashplate. The use of the servo-valve in place of the hydraulic servomotor and electric actuator used previously not only increases the frequency of the pair of complex roots but will also decrease the dead-band in the output speed regulation to a minimum. The root loci of this system were plotted in Fig. 29.

The compensation technique of Hsu [14] was applied to the vehicle model controlled by the servo-valve. The experimental results of the previous compensated system showed more damping than was predicted theoret-

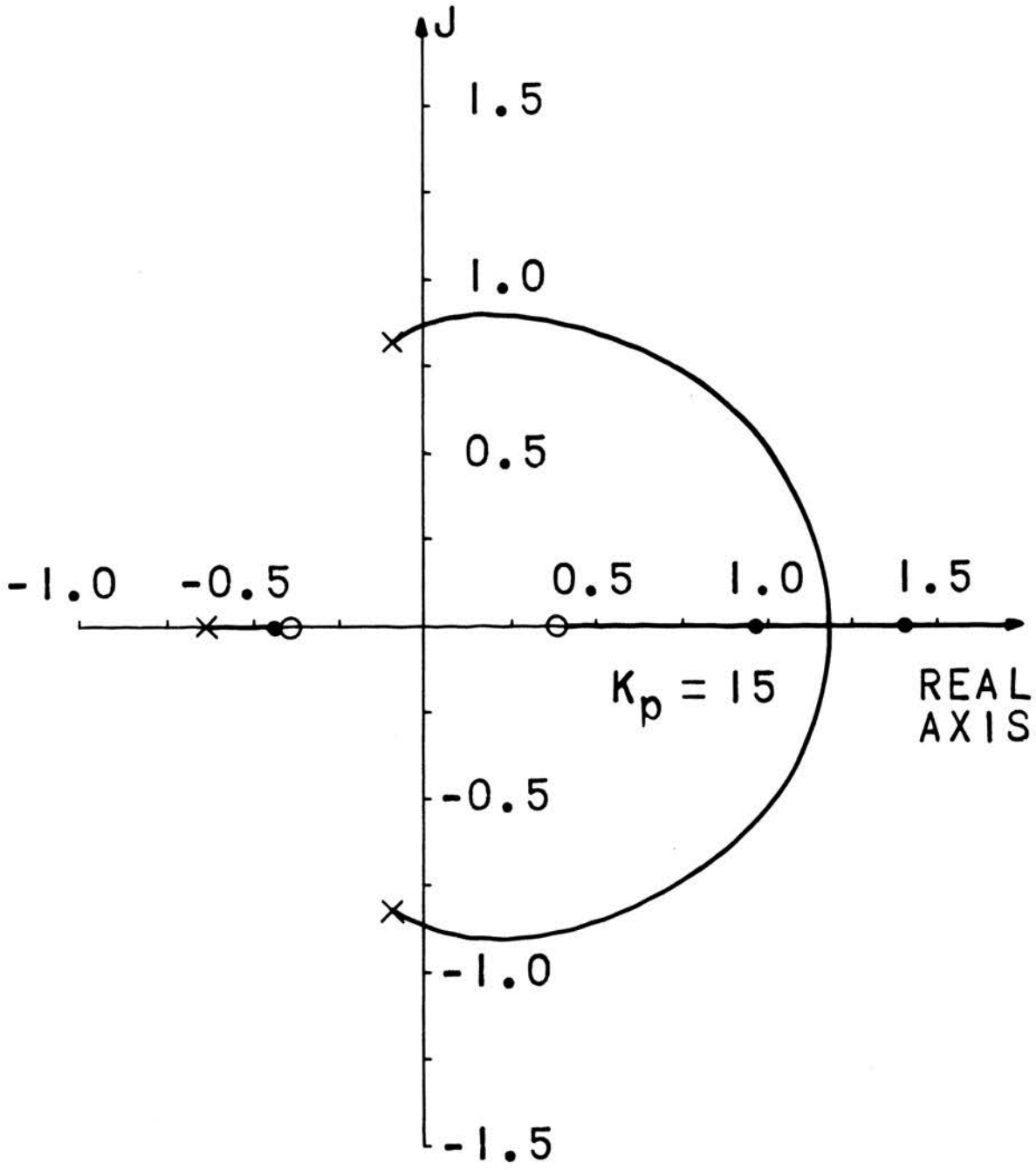

Figure 29. Uncompensated Vehicle Root Loci

ically. A smaller value of ζ was chosen for this design to permit a higher frequency for the roots of the system. In this case, when ζ was decreased from 0.3 to 0.25, an 18% increase in frequency was predicted. The design point was $-0.165 + j0.65$ and the compensator design was of the form

$$G_c(s) = \frac{(1 + \tau_z s)^3}{(1 + \tau_p s)^3} .$$

The partial root loci of the compensated system is shown in Fig. 30.

The damped frequency of the compensator roots which approximate the frequency of the engine speed control was 0.433. This corresponds to a cycle time of 14.5 seconds and the laboratory tests indicated (Fig. 24, 25, 26, and 27) that the output speed approached steady-state in approximately one half the engine speed control cycle time. The output speed of this system would reach steady-state in approximately 7.25 seconds.

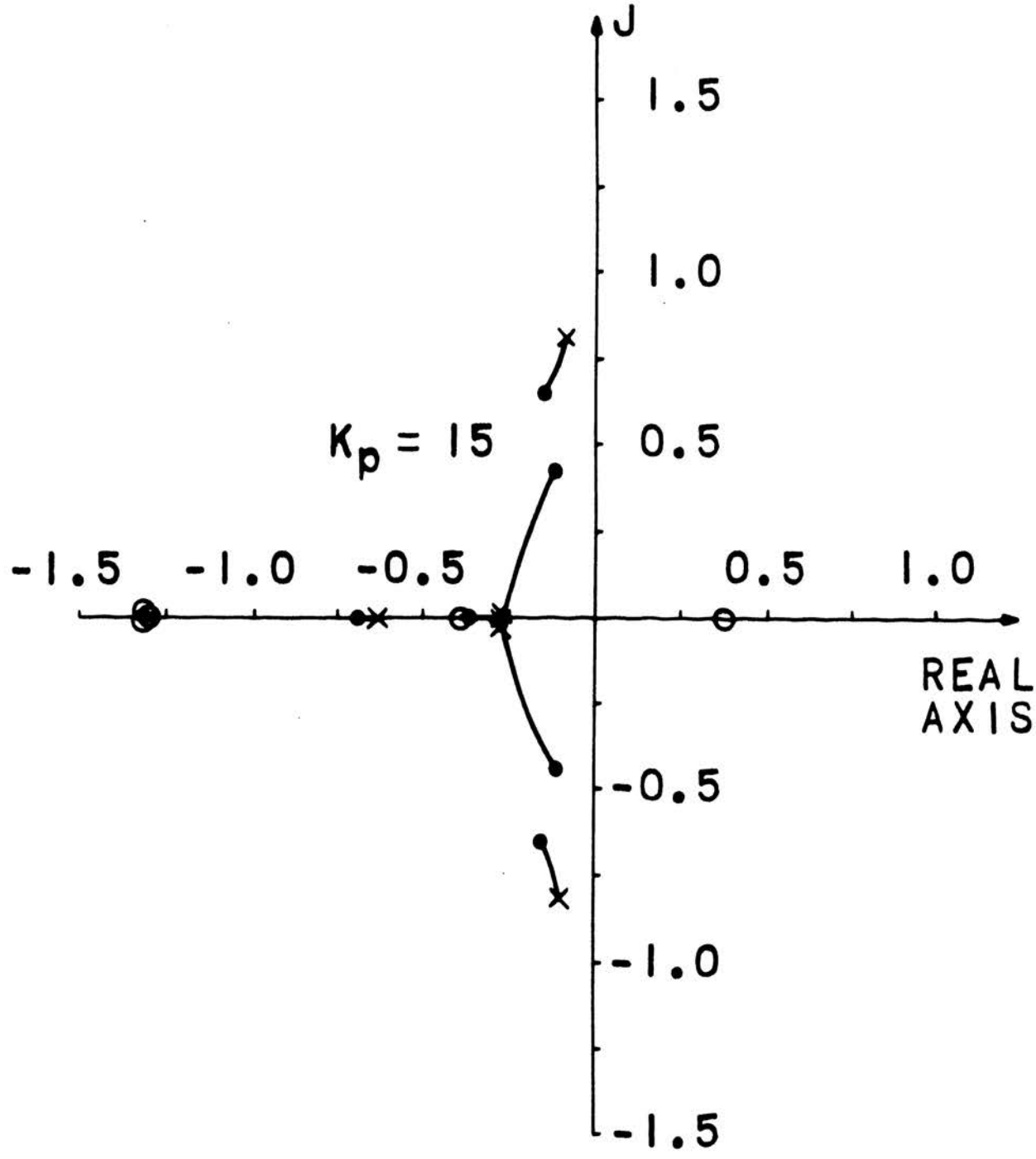

Figure 30. Compensated Vehicle Partial Root Loci

IV. CONCLUSION

The linear model of the engine, transmission, and dynamometer was sufficiently accurate for pre-fabrication design analysis. With this model to predict dynamic behavior, the positive feedback encountered in the engine speed control was successfully compensated. On the basis of the analytical investigation and the experimental tests, the following conclusions and recommendations were formed.

A. Conclusions

1. The output speed of industrial vehicles with hydrostatic transmissions could be satisfactorily controlled with the high gain and fast response of an electro-hydraulic servo-valve. This type control would be needed to correct the speed loss of the hydrostatic transmission.
2. The engine and motor speed could be satisfactorily controlled only when the power level is low a majority of the time, the frequency of the change in load is slow, and the ratio of engine inertia to vehicle inertia is high.
3. Electric motor operated actuators will not provide satisfactory speed regulation at low speeds because of the dead-band characteristics.

B. Recommendations

1. Investigate the stability of the system at the upper end of the minimum BSFC curve, i.e., operating between part load and full load conditions.

2. Experimentally determine the characteristics of the system using an electro-hydraulic servo-valve as the final control element.

3. Investigate a relationship for output speed regulation of the parameters $K_t/(\tau_t + \tau_{ta})$ vs. J_v/J_e.

V. BIBLIOGRAPHY

1. Killough, Walter W. "Construction Equipment Designers Aim to Lower Earthmoving Costs and Reduce Operator Effort," SAE Journal, September 1966, p. 81-3.

2. Wilson, Warren E. "Control Systems for Hydrostatic Transmissions," Machine Design, March 28, 1968, p. 141-4.

3. Raven, Francis H. Automatic Control Engineering, McGraw-Hill, New York, 1968, p. 648.

4. Wilson, Warren E. "Hydrostatic Transmissions," Machine Design, v. 33, December 7, 1961, p. 150-9.

5. Wilson, Warren E., Lemme, Charles D. "Hydrostatic Transmissions," HST Workshop, February 17-19, 1969, The Center for Professional Advancement, Hopatcong, New Jersey.

6. Johnson, Jack L. "Mathematical Modelling of Hydrostatic Transmissions," Delivered at NCFP Conference, October 18, 1968.

7. Howson, D. F. "The Case for Interconnected Engine and Pump Controls on a Tractor with Hydrostatic Transmission," J. Agric. Engng. Res., 9 (1964) No. 3, p. 288-93.

8. Latson, David M., Gordanier, Max, Dorgan, Robert J., Rio, Russell L. "A Hydromechanical Transmission Development," SAE Paper 670932, Combined Fuels and Lubricants, Powerplants and Transportation Meetings, Pittsburgh, Pa., October 30-November 3, 1967.

9. Lebedev, A. L. "Automatische Steuerung des Dieselmotors und des hydraulischen Schleppergetriebes," Landtech. Forsch. 17 (1967)

H. 6, S. 191/93.

10. SAE Handbook, Society of Automotive Engineers, Inc., New York, 1969.

11. Engineering Application Manual Bulletin 9565, Sunstrand Hydro-Transmission, LaSalle, Ill.

12. Eckman, Donald P. Automatic Process Control, Wiley, New York, 1962, p. 368.

13. Ross, E. R., Warren, T. C., Thaler, G. J. "Design of Servo Compensation Based on Root Locus Approach," AIEE Paper 60-779, AIEE Summer General Meeting, Atlantic City, N.J., June 19-24, 1960.

14. Hsu, C. C. "A New Graphical Method for Feedback Control System Compensation Design," AIEE Paper 62-78, AIEE Winter General Meeting, New York, N.Y., January 28-February 2, 1962.

15. Downs, M. E. "The Design of a Direct Current Generator Field Controller," Thesis, University of Missouri - Rolla, July 1969.

VI. VITA

Gordon Wright was born on September 9, 1941, in Qulin, Missouri. He received his primary and secondary education in Qulin, Missouri. He has attended the University of Missouri - Rolla, in Rolla, Missouri, from January 1963 to the present, receiving the Bachelor of Science degree in Mechanical Engineering in August 1966 and the Master of Science in Mechanical Engineering in January 1968.

He received a Caterpillar scholarship award for the Winter semester 1966 and from the Fall semester 1966 through the Summer semester 1969 held a National Defense Graduate Fellowship.

He was a self-employed farmer 1959 through 1962 and worked as a summer trainee at the John Deere Dubuque Tractor Works, Dubuque, Iowa, in the summer of 1965 and for Deere & Company Engineering Research, Moline, Illinois, in the summer of 1967. He has been employed by the University of Missouri - Rolla as a student assistant, graduate teaching assistant, and graduate research assistant.

He was married to Betty Carole Donica on December 19, 1959, and they now have three children; Charles, 8, John, 4, and Donica, 10 months.

VII. APPENDIX

A. Description of Electronic Sub-Systems. The control system equations developed are written below in Eq. (32) through Eq. (35).

$$N_{inc} = K_p(T_p - T_s) \tag{32}$$

T_s = engine torque set point

$$E_g = K_g(N_{inc} - N_{in}) \tag{33}$$

$$T_p = \frac{0.0418\ P\ R_i}{1 + 0.22D} + 0.00615\ N_p \tag{34}$$

$$E_t = K_t(N_{ms} - N_m) \tag{35}$$

To translate the model into a controller, the equations were patched on the analog computer. It was then necessary to scale the variables in order for their maximum values to be compatible with the maximum computer voltage. The scaled equations are

$$(0.01N_{inc}) = 0.04\ K_p\ [\ (0.25T_p) - (0.25T_s)\ ]$$

$$(E_g) = 100\ K_g\ [\ (0.01N_{inc}) - (0.01N_{in})\ ]$$

$$(0.25T_p) = 1.045\ (0.01P)\ \frac{R_i}{1 + 0.22D} + 0.153\ (0.01N_p)$$

$$(E_t) = 100\ K_t\ [\ (0.01N_{ms}) - (0.01N_m)\ ].$$

The system feedback signals were also scaled.

$$(0.01P) = \frac{0.01v\ 5000psig\ P_{tv}}{psig\ 22.7v} = 2.2\ P_{tv}$$

P_{tv} = Servionic H147-9 pressure transducer voltage

$$(0.01N_m) = N_{fb}$$

N_{fb} = governor shaft feedback potentiometer voltage

$$(0.01N_m) = \frac{1000\,\text{rpm}}{7\text{v}}\,TACH_m = 1.43\,TACH_m$$

$TACH_m$ = motor Servo-Tek No. SA-757A-2 tachometer feedback signal

$$(0.01N_p) = \frac{1000\,\text{rpm}}{7\text{v}}\,TACH_e = 1.43\,TACH_e$$

$TACH_e$ = engine Servo-Tek No. SA-757A-2 tachometer feedback signal

$$R_i = 1.88\,R_{fb}$$

R_{fb} = ratio lever feedback potentiometer signal.

The feedback quantities were then substituted into the scaled equations.

$$(0.01N_{inc}) = 0.04\,K_p\,[(0.25T_p) - (0.25T_s)]$$

$$(E_g) = 100\,K_g\,[(0.01N_{inc}) - N_{fb}]$$

$$(0.25T_p) = 4.33\frac{P_{tv}R_{fb}}{1 + 0.22D} + 0.219\,TACH_e$$

$$(E_t) = 100\,K_t\,[(0.01N_{ms}) - 1.43\,TACH_m]$$

The calculated input speed was limited between 0 and 15v. And the output voltages (E_g) and (E_t) were limited between ± 15v and ± 25v respectively. Also the commutation noise on the tachometer signals was filtered with a first order filter whose time constant was equal to 0.01 sec. The computer diagrams are shown in Fig. 31 with the parentheses notation for the scaled quantities dropped.

The power level of the computer output voltages, E_g and E_t, was not

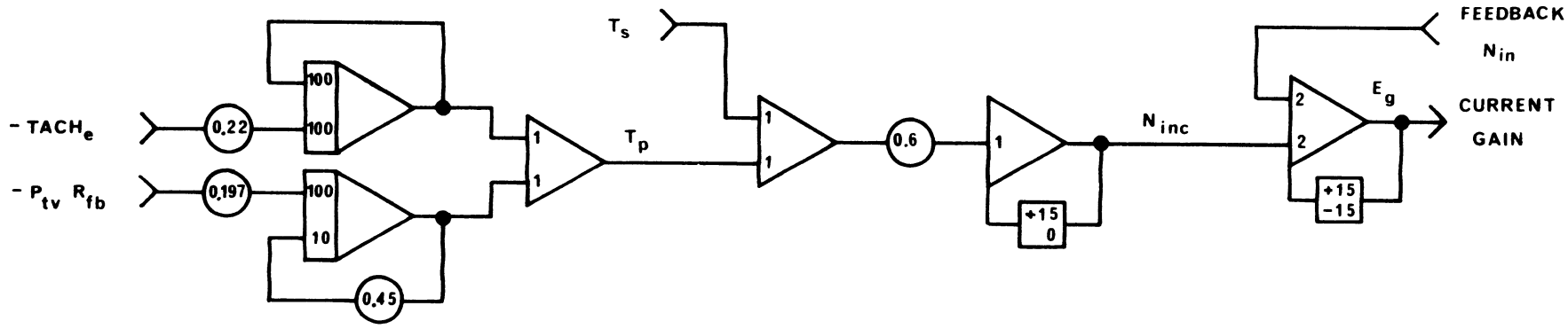

(a)

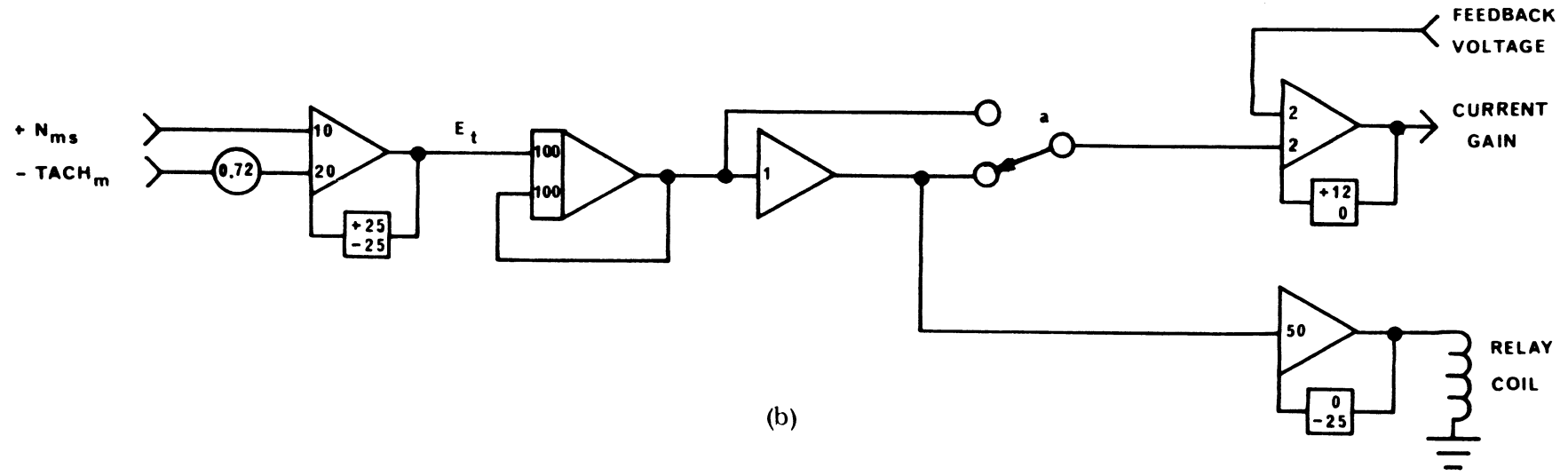

(b)

Figure 31. (a) Governor Controller Analog Computer Diagram; (b) Transmission Ratio Controller Diagram

sufficient to drive the actuator motors. It was necessary to have a current gain device between the computer and the actuators. A Hewlett-Packard amplifier was used in the governor control loop. And a device was constructed by the author for the transmission ratio controller. A diagram of this current gain device and the actuator is shown in Fig. 32. Since this device was capable of only positive output and input, a four channel relay was used to provide direction reversal for negative E_t. Channel "a" kept the input positive, channel "b" connected the motor through the appropriate limit switch, and channels "c" and "d" reversed the field polarity.

The computer diagram for the compensator

$$G_c(s) = \frac{(1 + \tau_z s)^2}{(1 + \tau_p s)^2}$$

is given in Fig. 33 with $\tau_z = 1.175$ and $\tau_p = 12.5$.

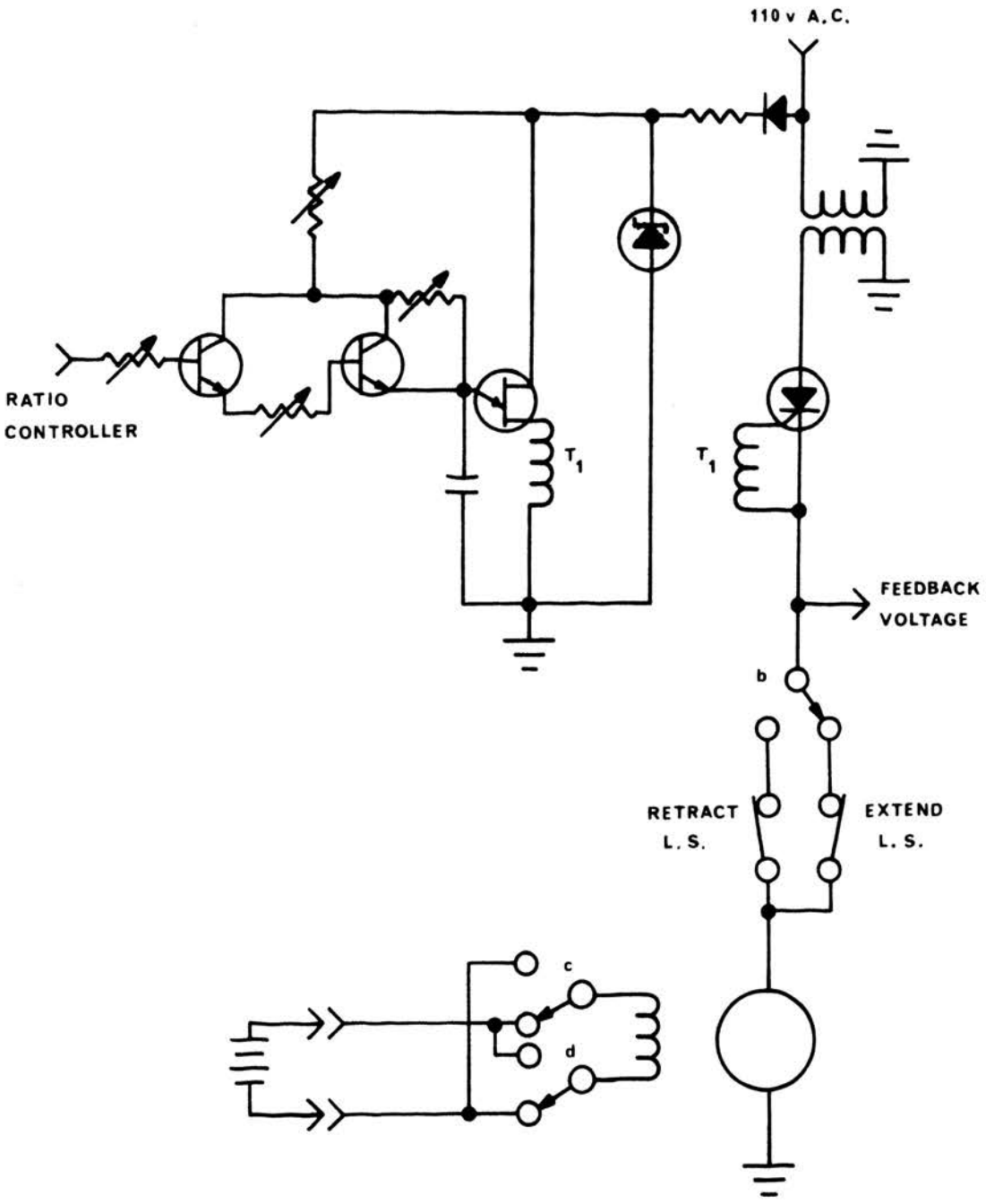

Figure 32. Transmission Ratio Controller Current Gain Device and Actuator

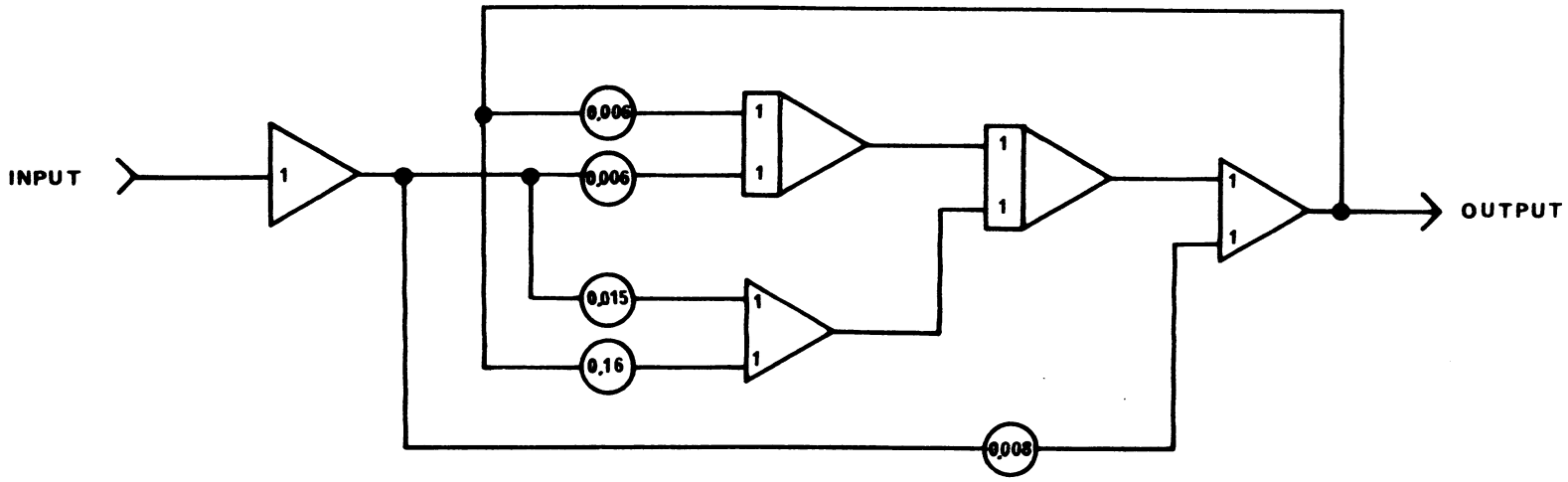

Figure 33. Analog Computer Diagram for the Compensator